Fluid Mechanics of Bubble Capture by the Diving Bell Spider

by

Alice Brooks

Submitted to the Department of Mechanical Engineering in Partial
Fulfillment of the Requirements for the Degree of
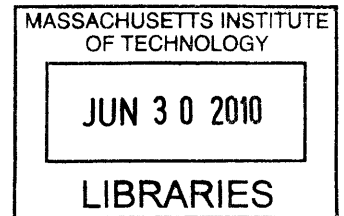
Bachelor of Science

at the

Massachusetts Institute of Technology

June 2010

© 2010 Alice Brooks

Signature of Author.............

Department of Mechanical Engineering
May 10, 2010

Certified by..
Dick K.P. Yue
Philip J. Solondz Professor of Engineering
Thesis Supervisor

Accepted by......
John H. Lienhard V
Collins Professor of Mechanical Engineering

Fluid Mechanics of Bubble Capture by the Diving Bell Spider

by

Alice P. Brooks

Submitted to the Department of Mechanical Engineering
on May 10, 2010, in partial fulfillment of the
requirements for the degree of Bachelor of Science in
Mechanical Engineering

Abstract

The water spider, a unique member of its species, is used as inspiration for a bubble capture mechanism. Bubble mechanics are studied in the pursuit of a biomimetic solution for transporting air bubbles underwater. Careful experimentation is performed to understand the mechanics of bubble formation and capture.

Investigation of bubble formation through an underwater nozzle shows that bubble volume increases by 15% when parallel rods are spaced above the nozzle at the same width as the inner diameter of the nozzle. Bubble volume decreases linearly with increasing air injection rate. Decreasing surface tension by approximately 40% decreases bubble volume by approximately 20%. Changing the angle the nozzle from parallel to perpendicular with the bottom of the tank increases bubble volume 40%.

Based on trends observed in the nozzle experiments and using the spider's mechanisms for bubble capture as inspiration, a bubble capture device is manufactured. Decreasing the surface tension of the fluid by 25% decreases captured bubble volume by 50%. Below a device submersion speed of approximately 2.4 mm/s, bubble formation was at a maximum for the device, regardless of fluid surface tension.

This research elucidates the limitations on bubble capture by the water spider. For future applications, these limitations can be pinpointed and adjusted for more efficient bubble capture and plastron maintenance.

Thesis Supervisor: Dick K.P. Yue
Title: Philip J. Solondz Professor of Engineering

Acknowledgements

Table of Contents

List of Figures

List of Tables

List of Symbols

D	Inner diameter of nozzle (mm)
d	Rod spacing (mm)
s	Submersion speed (mm/s)
s_0	Standard submersion speed (mm/s)
v	Volume (microliters)
v_0	Standard volume (microliters)

11

1 Introduction

The water spider, or *Argyroneta aquatica*, is a unique member of its species that lives its whole life underwater. When swimming, the water spider breathes through a plastron around its abdomen (Flynn 2008). The spider is intriguing because of its ability to transport large bubbles of air, relative to its size, below the surface of the water to create the underwater habitat.

Multiple studies have examined plastron respiration (Thorpe 1950, Schutz 2003, Shirtcliffe 2006, Flynn 2008). Few have looked to the water spider and it's mechanism of bubble capture as inspiration for other applications. Biomimicry is a popular method for creating new solutions to problems that have previously gone unsolved. Taking a closer look at the water spider could provide solutions for new hydrophobic materials, underwater devices that require insulation, or new methods by which to prevent corrosion.

Biomimicry of the mechanism by which the water spider transports bubbles underwater is a complicated problem, one that requires division into more straightforward parts. Before the behaviors of the spider can be mimicked, the underlying principles and conditions must be explored and understood.

The study started with an examination of the characteristics of bubbles emitted from an underwater nozzle. The surroundings of the nozzle opening, rate of air injection into the nozzle, fluid surface tension, and angle of the nozzle from the horizontal were varied, with the goal of describing and implementing conditions for maximum bubble volume given certain conditions.

Several hypotheses were formulated concerning the behavior of bubbles emitted from the underwater nozzle when subjected to changing conditions.

1. Parallel rods positioned on the sides of the nozzle increase bubble volume.
2. Rod diameter does not affect bubble volume.
3. Slow air injection rate into the nozzle corresponds to greater bubble volume.
4. Lowering the surface tension of the surrounding fluid decreases bubble volume.
5. The further the nozzle is positioned from perpendicular to the bottom of the tank, the smaller the bubble volume will be.

These hypotheses were each addressed with a unique experiment, as detailed later in Methods.

Conclusions from the underwater nozzle study were used to formulate a set of hypotheses in the development of a passive bubble capture device. The bubble capture device provides greater insight into the extraordinary way by which the water spider survives underwater. The underwater nozzle study illuminates some of the effects of environmental changes, but the bubble capture device more closely shows the effects of changing environmental parameters on the volume and shape of the bubble as it would be captured by the aquatic organism.

Again, several hypotheses were developed. Experimental methods were developed in order to provide answers and insight into each of the following hypotheses.

1. Decreasing surface tension decreases the bubble volume that can be captured in the device. Surface tension and bubble volume have a non linear relationship, with a small change in surface tension having a much greater effect on bubble volume.
2. Below a critical submersion speed, bubbles form at the maximum value. In an intermediate speed range, bubble volume decreases. Above another critical speed, bubbles do not form.
3. The device has certain physical and geometric requirements for bubble capture.
    a. Coated rods capture larger bubble than uncoated rods.
    b. A hydrophobic sponge is necessary for bubble capture.
    c. A larger hydrophobic sponge captures a larger bubble.
    d. More than two rods forming the device are necessary to achieve passive bubble capture. Structures made with increasing number of rods are shown in Section 4.2.3.

Again, the hypotheses are all addressed in the Methods section, with details a description of how each was approached. Background provides the basis on which many of these hypotheses were formed. Others were the result of benchmark testing. Methods will detail how the hypotheses were addressed. Results and Discussion will confirm or falsify the assertions made in the Introduction. The Conclusion section will synthesize the results and frame the hypotheses in the larger picture, giving suggestions into how these questions and their results can be used for other applications.

2 Background

2.1 The water spider

As briefly discussed in the introduction, the water spider is a unique member of its species. The water spider lives exclusively in northern Europe and Japan. It can only be found in freshwater, in areas shielded from fast flows and currents (Flynn 2008). Studies that have gone into understanding its behavior (Schutz 2003, Shirtcliffe 2006). Strict import laws into the United States have prevented many from further study of the water spider. There are many aspects of the water spider that make it exceptional, starting with where it lives.

2.1.1 Life underwater

The water spider lives its entire life underwater. It stays for long periods in a diving bell-like habitat underwater. First, the spider weaves a web amongst water plants in shallow, slow moving freshwater. As the web is hydrophobic, it traps air bubbles that the spider releases from below. These bubbles merge into a large bubble suitable enough for the spider to eat, lay eggs, and sleep in for a month at a time (Flynn 2008). The isolated environment also protects the water spider from predation. Oxygen produced by the water reeds diffuses through the fluid gas interface, limiting the necessary number of trips to replenish oxygen stores (Schutz 2003).

Schutz found that the water spider uses its underwater habitat as an external lung. Female water spiders were studied as they spend a greater percentage of their lives in the bell than males. Air within the bell was replaced with pure oxygen, pure carbon dioxide, or ambient air and the response of the spider observed. When carbon dioxide was injected, spiders surfaced to replenish the air supply more often than with oxygen and added to the web to create a larger bell. It was concluded that the water spider does monitor oxygen concentration and breathes the air in the diving bell (Schutz 2003).

2.1.2 Water spider bubble capture

The water spider fills its habitat with air through a unique bubble capture process. It gathers air from the water surface using its hind legs. In a sharp movement, the spider captures air between its back most legs and uses its other set of hind legs to detach the air bubble and take it underwater (Schutz 2003). Figure 1 shows the spider in the process of bubble capture.
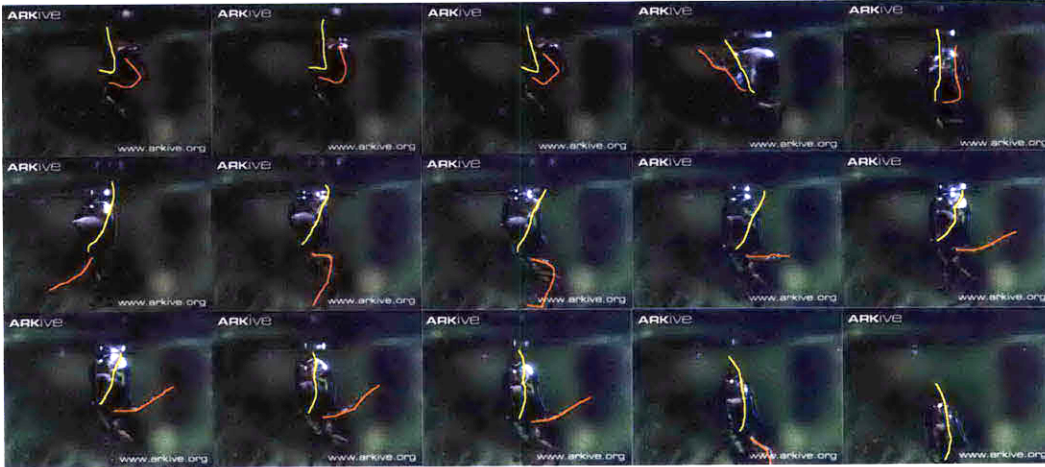
Figure 1: Video stills of spider detaching air bubble from the surface of the water (ARKive). The yellow line represent on of the legs in the backmost pair. The orange line represents another leg. The spider uses the yellow set of legs to create a frame for the bubble. The orange legs kick through the interface of water and air, separating the bubble. The spider uses the yellow set of legs to hold the bubble as it swims underwater.

These stills are taken from a video from the (ARKive). In the side view, one leg from each of the two hind pairs of legs is highlighted. The yellow line corresponds to the backmost set of legs. The orange represents the next set of legs. The yellow legs are used to create a frame for bubble capture. The water spider sticks the yellow legs out of the water, and then lowers them down almost completely through the fluid air interface. In a sharp motion, the orange legs kick through this interface while at the same time the abdomen is slightly lowered. This combination of kicking and lowering the body is essential to separate the bubble. The spider then struggles with buoyancy, stabilizing itself while holding onto the bubble with its backmost legs. The yellow pair must stay vertical around the abdomen to keep the bubble from escaping to the surface. The front three set of legs are required to work together to overcome the buoyancy in order for the spider to swim back to its web.

2.1.3 Water spider breathing

When swimming, the water spider breathes through a plastron around its abdomen (Flynn 2008) The plastron is maintained passively. The hydrophobic properties of the coating on the spider's abdomen and the geometry of hair arrangement prevent complete wetting. With incomplete wetting, there is always a layer of air between the spider's abdomen and the surrounding water that the spider can breathe through.

Oxygen is taken in through spiracles along the spider's abdomen. These spiracles are positioned among the dense layer of hairs on the abdomen. Flynn et al took images of these spiracles, also proving that they are never touched by water (Flynn 2008).

Shirtcliffe et al modeled the plastron of the spider and confirmed that it does breathe through the plastron. A hollowed out cylindrical block of sol-gel foam was used for experimentation. The hydrophobic surface of the foam allowed a passive layer of air to form along its surface. This air layer was used to mimic the plastron of the water spider. The block was submerged, with an oxygen sensor in its center cavity submerged in water. Oxygen levels were monitored

over time to determine if oxygen diffusion occurred across the air layer on the outside of the block. It was concluded that oxygen levels necessary for survival could be obtained (Shirtcliffe 2006).

2.1.4 Water spider anatomy

Adult *Agyroneta aquatica* are typically 8-15 long (ARKive). Another feature that sets the water spider apart from other species of spiders is that it exhibits reversed sexual size dimorphism. As female size is limited by the energetic cost of building air bells, they are usually smaller than the males. Females must expend more energy as they build larger bells in which they live for longer periods of time to take care of their young. Since males spend more time hunting and swimming, larger bodies are required for better locomotion. For females, who spend more time building air bells, air bell size is directly related to body size (Schutz and Taborsky). Both males and females have legs about the length of the body or longer (ARKive).

Figure 2 shows an average size water spider. From the tip of the head to the abdomen, the average water spider is 12 mm in length. Back legs are approximately 16 mm in the figure below.
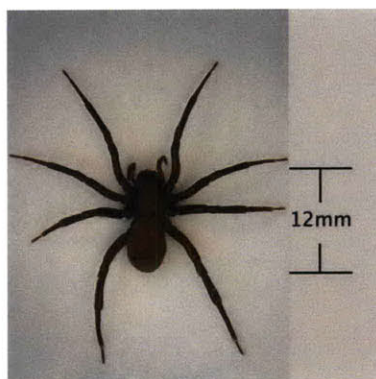
Figure 2: Water spider anatomy (ARKive)

2.1.5 Surface features and hydrophobicity of the water spider

As described in the earlier section, the water spider breathes through spiracles on its abdomen. The spiracles obtain air through the thin layer of air that is always coating the spider's abdomen. This plastron is maintained passively. The hydrophobic properties of the coating on the spider's abdomen and the geometry of hair arrangement prevent complete wetting of the surface of the abdomen. When incomplete wetting occurs, it is referred to as the Cassie state (Cassie 1944). The Cassie state occurs when it is more costly energetically for a surface to be wetted than for the liquid to be separated from the surface by a layer of air. Figure 3 shows the difference between the Cassie (partially wetted) and Wenzel (completely wetted) states.
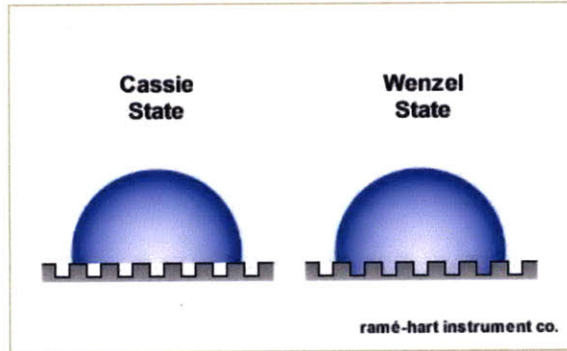
Figure 3: Cassie and Wenzel states of wetting (Ramé-Hart)

Key to the wetting properties of such a surface is the asperity height relative to the spacing between asperities. In organic surfaces, this ratio is described by the surface roughness. The surface of the water spider displays two levels of surface roughness. Similar to water walking insects, the abdomen of the spider is coated with a rough waxy material. Hairs spring from this surface, creating two scales of roughness (Flynn 2008).
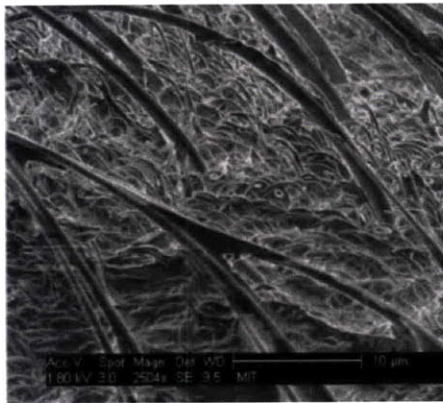
Figure 4: Surface detail of water walking insect (Flynn 2008)

Using the Young Laplace equation, Flynn et al derived an equation relating minimum asperity height to contact angle and geometry. By studying gas concentrations and pressures in the plastron they concluded that the liquid air interface around the spider was sufficient for oxygen diffusion (Flynn 2008).

The surface of the water walking insect is similar to the surface of the lotus leaf, a superhydrophobic surface, which upon microscopic inspection reveals two scales of surface roughness (Barthlott 1997).
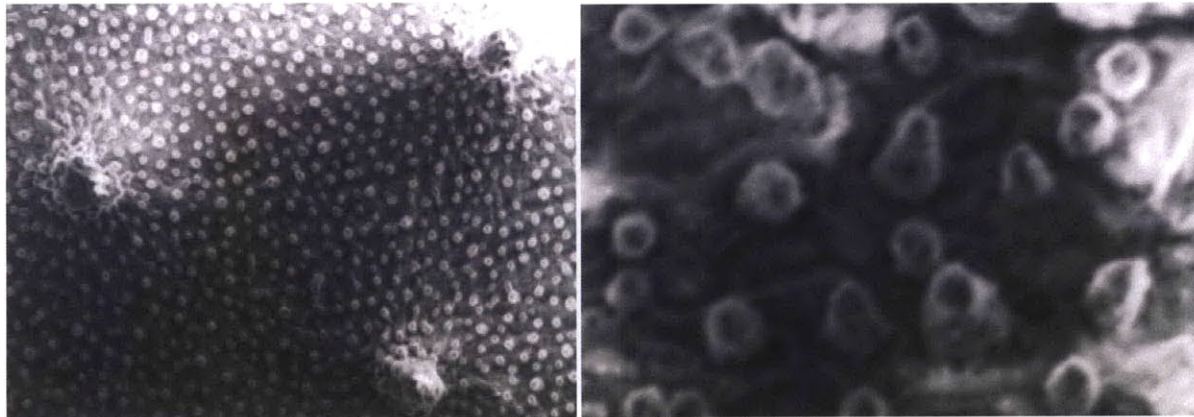
(a) (b)

Figure 5: SEM images of lotus leaf taken by the author in the course 2.674 in the 2.674 teaching laboratory at MIT, (a) larger scale, 2 levels or roughness are visible, (b) smaller scale roughness

Images were taken using an SEM in the 2.674 teaching laboratory at MIT. Scaling readouts on the microscope were faulty at the time measurement so exact magnification is unknown. Figure 5a is at lower magnification. Here, the two scales of roughness are visible. Research has shown that roughness is a key feature of hydrophobic surfaces. Two scales of roughness increases hydrophobicity.

Extrand et al showed that critical asperity height is directly proportional to the maximum distance between asperities and the tangent of the apparent contact angle. Contact angle is dependent on material properties. In order to maintain the Cassie state, the asperity height must be above this critical value (Extrand 2004).

Herminghaus showed that while steep indentations in a surface can suspend liquid and prevent wetting, adding smaller scale surface roughness requires less steep indentations (Herminghaus 2000). This added roughness makes it more costly energetically for water to permeate all surfaces. The degree of wetting depends on the geometry of this roughness and material properties such as contact angle. Contact angle is directly related to surface tension.

The contact angle of a material can be greatly increased by roughening. The wax of certain plant leaves has a contact angle of approximately 90° when smooth, but when rough, the contact angle doubles, making the leaves superhydrophobic (Herminghaus 2000).

According to Wenzel, the roughness factor is a ratio between the surface area of a rough surface and the surface area of a smooth surface with same shape and dimensions. The roughness factor is related to equilibrium contact angle by the specific interfacial energies of the solid and liquid (Wenzel 1949). Wenzel acknowledged that the exact roughness factor is unclear and not defined by a simple ratio.

Over time, contact angle can change. In a phenomena called hysteresis, contact angle decreases over time and wetting increases. Minimum hysteresis is desired for a surface to retain hydrophobicity. It has been shown that particular plant leaves lose hydrophobicity when submerged in water for a period of time due to hysteresis. (Herminghaus 2000). Certain aquatic arthropods avoid this problem by never allowing water to contact parts of their surface, thus avoiding hysteresis.

Water insects that have adapted to underwater life will retain a constant volume of air on their hairy abdomens, not undergoing hysteresis (Thorpe 1950). Many aquatic arthropods combine a rough waxy surface coating with dense hairs to achieve water repellency (Flynn 2008). Argyroneta aquatica combines a lower waxy coating of hair with large thicker rough hairs. These two levels greatly decrease solid fraction of their surface area. Its abdomen is densely coated with hairs. There are also larger hairs protruding from the surface. They are rough and coated with hydrophobic secretions

2.1.6 Biomimicry for superhydrophobicity

The water spider can be used for inspiration for the development of new material technologies. Biomimicry is often used to create new technologies. Often, the best solutions to a problem can be found in nature as they have developed over the course of the evolution of the organism.

Research has been done at MIT to mimic the Namib Desert beetle to create self-cooling computer chips (Zhai 2006). The lotus leaf has also been mimicked to create self-cleaning windows, non-corrosive piping, drag reducing surfaces, and many other applications (Abbott 2007).

2.2 Bubble mechanics

With the increasing availability of high speed cameras, there have been many recent studies observing and documenting bubble behavior during emission from an underwater nozzle. A literature survey was performed to get a sense of what type of research has been performed in recent years in the field of bubble emission form an underwater nozzle. Bubble shape around and at the moment of pinch off (Longuet-Higgins 1991, Oguz 1993, Thoroddsen 2007), characteristics of the pinch off surface (Keim 2006, Fontelos 2009), and bubble pinch off in fluids of varying viscosities have all been studied (Burton 2005).

Longuet-Higgins et al published the earliest of these studies. They measured the maximum bubble volume that could be emitted from nozzles of varying diameter. A bubble emits an acoustic pulse at pinch off from an underwater nozzle. This acoustic pulse was used to determine the exact volume of the bubble at pinch off. A high speed camera was also used to record the sequence of bubble shapes before and after pinch off.

Figure 6: Recorded images of bubble pinch off, nozzle inner diameter 4.00 mm, and film speed 2000 frames/second (Longuet-Higgins 1991).

They found that the radius of the bubble is simply related to the acoustic frequency, and that observing acoustic frequency provided the most accurate measure of bubble volume. Also, rate of air flow into the bubble was the key parameter for bubble volume.

A decade and a half later, Thoroddsen et al captured crisper images of the bubble at pinch off. The figure below is from their 2007 paper.
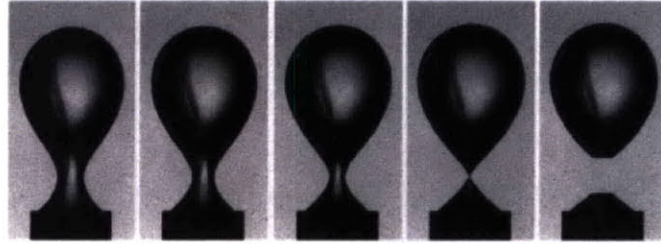
Figure 7: Bubble emitted from an underwater nozzle at pinch off, 0.5 ms between frames.
Inner diameter of the nozzle is 2.70 mm. Outer diameter is 3.14 mm. (Thoroddsen 2007).

After observing the images of bubble pinch off collected by Longuet-Higgins et al, Oguz et al developed a model for the growth of a bubble from a submerged needle. They formulated a model for bubble growth, dependent on whether gas flow rate into the bubble was above or below a critical value (Oguz 1993). Theoretical bubble shapes were also calculated and compared with the images from Longuet-Higgins et al.

Keim et al also used high-speed video to study air bubbles detaching from an underwater nozzle. They studied the shape of the neck just after pinch off. It was concluded that air in water retains a spatial memory of initial conditions after pinch off, retaining any asymmetries in the bubble collapse (Keim 2006).

Using a high speed camera of 100,000 frames per second, Burton et al studied the pinch off of bubbles in fluids with a wide range of viscosities. Nitrogen gas was used for the bubbles. Differences in neck shape before pinch off were observed, with a more parabolic shape characteristic of the gas in high viscosity fluid (Burton 2005).

Fontelos et al performed analysis on the bubble at pinch off, finding a time dependence of the minimum radius of the pinching neck. Also, they developed a spatial model of the neck at pinch off. Experimental results were compared to the model, resulting in good agreement.

Still unexplored by all of the studies explored above are methods by which to increase the volume of a bubble emitted from an underwater nozzle before pinch off. This goal is a main focus of experiments detailed in the first half of the current study.

2.3 Surface tension

2.3.1 Role in life of the water spider

Similarly, in the study of plastrons form around water spiders and other arthropods, the interaction between the fluid and gas is critically dependent on surface tension. As stated in the description of the Cassie and Wenzel states, surface tension is responsible for the forces that prevent wetting. When surface tension forces are overcome, wetting occurs.

Flynn et al studied the role of surface tension at the fluid gas interface on the plastron of water arthropods. They found that surface tension is the critical factor in the formation of the plastron (Flynn 2008). Without the plastron the water spider would not be able to breath underwater. Surface tension also keeps the spider's underwater habitat from breaking apart. The water spider deposits air bubbles into an underwater web. If surface tension were lowered, air would escape between the threads of the web.

2.3.2 Effect of pollutants on surface tension

Pollutants can have a drastic effect on the surface tension of a body of water, severely altering conditions for the wildlife that lives in the water. Pollutants typically lower the surface tension of a fluid. Water walking insects will lose the ability to walk across the surface of water as shown in the figure below.

| Distilled Water (Control) | 0.001M | 0.002M |
| 0.003M | 0.004M | 0.005M |
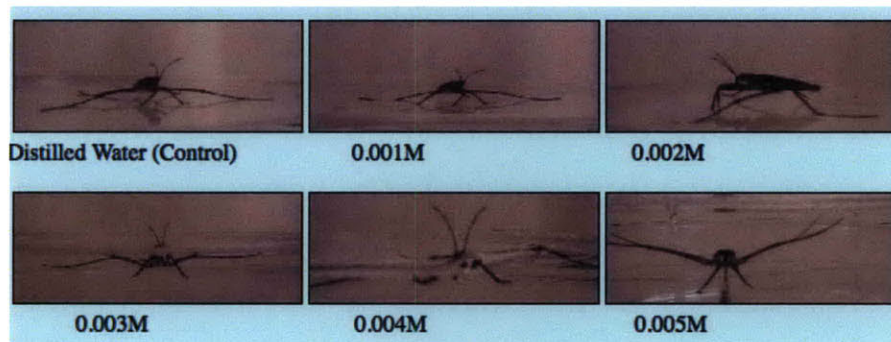
Figure 8: Water striders walking on water surface with varying surface tension (WWLPT)

The insect in the photos ceases to be able to walk on the water when the surface tension decreases below a critical point. When 0.003 molar of the surfactant is added, the water strider is no longer supported.

Another organism that is drastically affected by drops in surface tension is an aquatic bird. Decreased surface tension allows wetting of the plumage. The bird uses the plumage for insulation against the cold. With normal surface tension, the plumage does not wet, allowing for a layer of air to be trapped against the body of the bird. When wetting occurs, the bird must expend much more energy in order to maintain body temperature levels and avoid death (Stephenson 1997).

In addition, environmental studies have been performed using surface tension measurement as an indicator for pollution in bodies of water (Larumbe 1987).

2.3.3 Scaling effects of surface tension

Shirtcliffe et al, who studied the gas diffusion properties of a plastron, postulated that the plastron could be scaled up to a volume large enough to sustain breathing for a human. This human size plastron would have a diameter of 2.8 m surface area of 90 m^2. (Shirtcliffe 2006). There are many more complicated issues that arise when considering creating on the large scale what has only been previously observed on a much smaller scale. Buoyancy would have a large effect on the locomotion of a body of this size. The force required to overcome buoyancy might be so costly energetically as to outweigh the benefits of maintaining the plastron.

3 Methods

Two broad sets of experiments were performed in order to further understand the mechanisms by which the water spider captures and holds bubbles to transport underwater. The first set of experiments studied the statics of a bubble emerging from an underwater nozzle. Bubbles were of approximately the same volume as those captured by the water spider. Parameters of the experiment were varied to determine conditions for maximum bubble volume emission.

The second set of experiments studied the effects of varying conditions surrounding a passive bubble capture device. The device signifies development towards more pinpointed mimicry of the method by which the water spider brings air bubbles underwater. The device was built to bring together both the typical bubble volume from the previous experiments and the action of capturing the bubble.

In the analysis of the measurements taken in the experiments, measured values were non dimensionalized for their presentation in Results. Measured values were made dimensionless so that findings could potentially be applied to other systems. Dimensionless bubble volume, v/v_0 which is plotted on the y axis in most of the graphs, was obtained by dividing the measured bubble volume v by a standard reference volume v_0. The standard value used for v_0 is given along with every graph.

3.1 Underwater nozzle experiments

As described in Section 2.2, many studies have examined the dynamics of bubble formation and pinch off from an underwater nozzle. High speed photography has been used to obtain precise images of bubbles in millisecond intervals during bubble pinch off. The shape of the neck of the bubble as it separates from the nozzle has also been examined. What all of these studies lack is an examination into the possibility of increasing the volume of the bubble emerging from the underwater nozzle.

3.1.1 General Experimental Set Up

A clear plastic tank was used in all the following experiments. The tank was 16 cm long, 8 cm wide, and 5 cm tall. Unless otherwise stated, for each experiment, the tank was filled with approximately 300 mL of tap water in the range of 20 to 24 degrees Celsius. Temperature measurements were always taken at the start of each set of experiments, sometimes for each data point. Recorded temperatures were never outside of the given range, which is referred to as room temperature.

A nozzle was constructed from a plastic straw. The inner diameter of the straw was 4.3 mm with a 0.45 mm wall thickness, which resulted in a more rigid straw then common drinking straws. Preliminary testing was performed with a variety of nozzle sizes to determine which would give the best visuals of bubble emission. The nozzle selected had more of the air bubble visible than a larger nozzle.

The straw was cut to 2 cm length. A hole was punctured through one of the walls 5 mm down from the top of the straw. A pin was used to puncture the hole. The hole was used as the site for air injection through a syringe. A 10 microliter syringe glass Hamilton syringe was used for air injection. Measurements on the side of the syringe were accurate to 0.1 microliter. After the hole was made in the nozzle, the syringe was inserted and removed repeatedly to insure easy insertion and removal later during experimentation. Multiple air injections from the syringe were needed to create a bubble large enough to detach from the nozzle.

Before each insertion of the syringe, it was filled to capacity with 10 microliters of air. Air was injected in the nozzle at a low flow rate, approximately 2 to 4 microliters per second, unless otherwise stated. For bubbles of volume greater than 10 microliters, the syringe was emptied, refilled, and reinserted. The process was repeated until the bubble reached pinch off.

Rigidity of the nozzle was a key characteristic for repeatable air injection. The straw did not deform under the pressure from the nozzle during insertion and removal. The nozzle was affixed to the bottom of the tank using putty. The putty created an air tight seal. There were no signs of air leakage through the putty when air was injected into the nozzle. The putty did not adhere to wet surfaces, so the nozzle was positioned in the tank before any fluid was added.

Below is a photograph of the general nozzle set up.
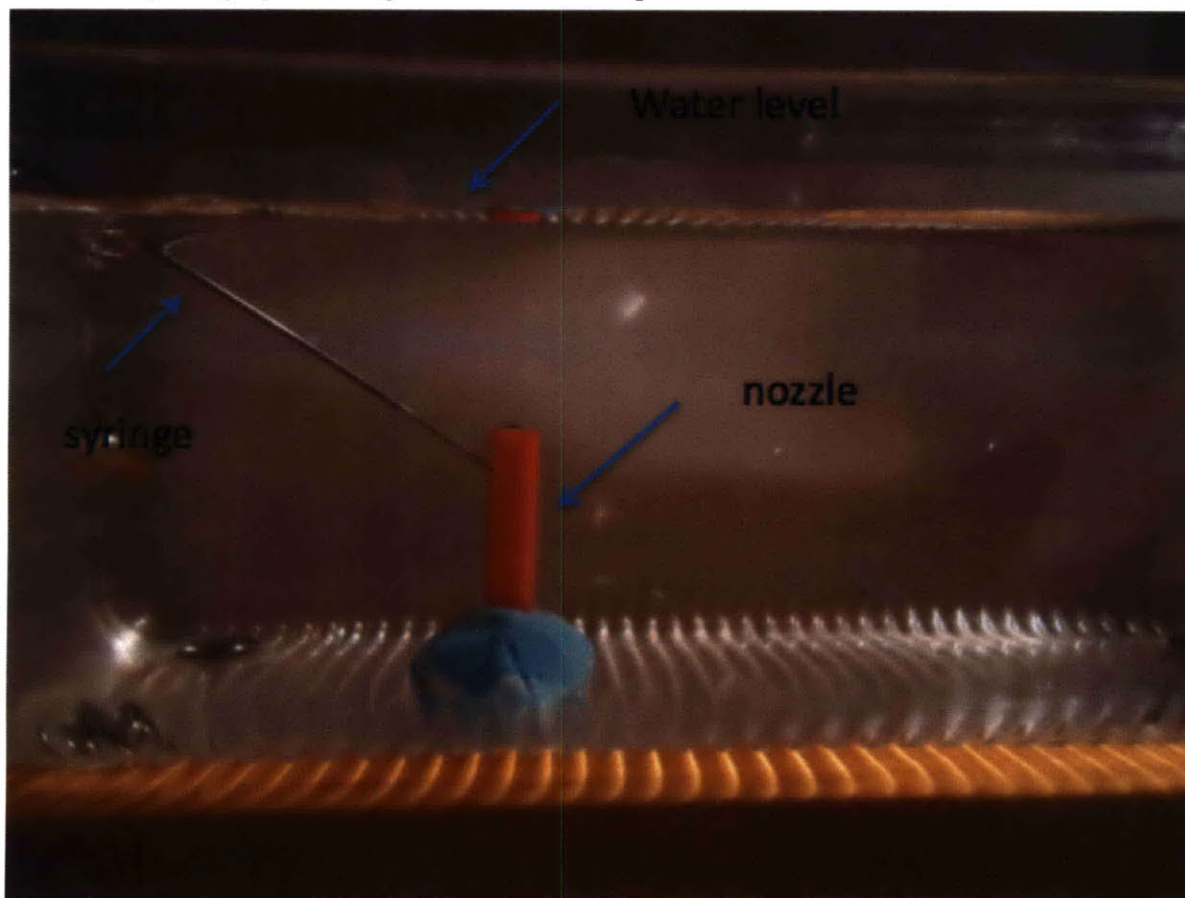
Figure 9: General experimental set up for nozzle experiment. Plastic nozzle is attached in airtight seal to the base of the tank. Water level is approximately 2 cm above the opening of the nozzle

Bubble volume was recorded directly from the syringe. Measurements were reported to 0.1 microliter accuracy. As bubble pinch off occurred, air injection was ceased and the total volume injected was recorded. Because of the very low injection rate of the air, injection could be ceased very close to the exact moment of bubble pinch off. A standard digital camera was used to capture images of the bubbles exiting the nozzle.

Unlike the work performed by Longuet et al, the following experiments modified the conditions the bubbles faced as they exited the nozzle. These conditions are described in the following sections.

3.1.2 Effect of side rods

Parallel aluminum pins were chosen to mimic the back legs of the water spider. Figure 1 in the Introduction shows that the extension of the legs around the abdomen of the spider is essential for capturing the volume of air. The legs are extended vertically and parallel to each other. For the current study, pins typically used for sewing were chosen to mimic the legs of the spider.

3.1.2.1 Rod spacing

Rods were placed vertically above the nozzle. One rod was super glued to each claw of a caliper. This allowed for quick changes in rod spacing while maintaining the rods at parallel to each other and the sides walls of the nozzle. Opening and closing of the calipers altered the distance between the rods the same amount. The digital read out on the calipers made spacing simple and reliable to record. Distance between the rods was also verified with another caliper at spacing changes for added certainty. Spacing was varied between the nozzles from 0 to 5 mm.

The bottom tips of the rods were positioned at the top of the nozzle. The center of the space between the rods was positioned approximately above the center of the nozzle.
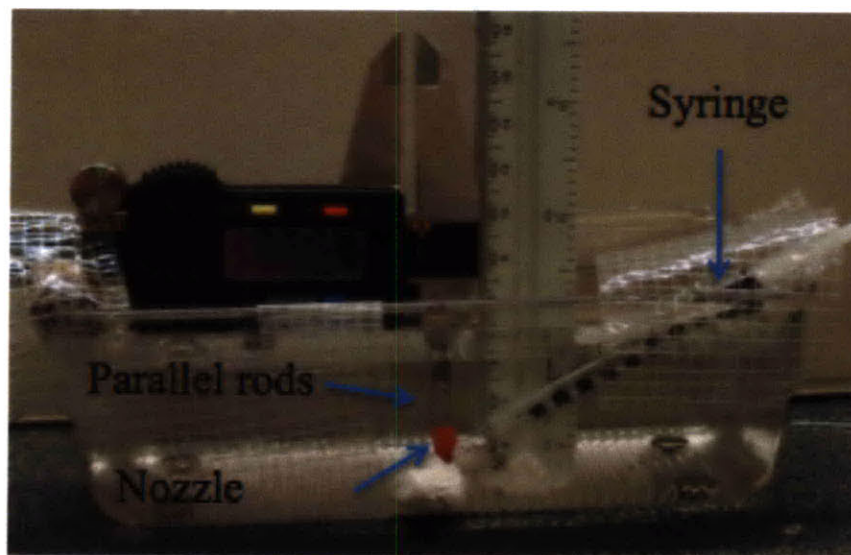
Figure 10: (a) Experimental set up for rod spacing experiment. Rods are glued parallel to each other on the calipers, and placed directly above the nozzle. Air is injected through a syringe into the nozzle. A ruler is placed next to the nozzle for reference

3.1.2.1 Effect of rod texture

The sewing pins were replaced with bristled rods to test the effect of rod texture on bubble volume. Spacing was varied as with the previous rod spacing experiment, but all other parameters were kept constant.

3.1.2.2 Effect of rod diameter

Rods of varying diameter were spaced 4.3 mm apart and positioned directly above the nozzle. For each set of rods, a bubble was emitted from the nozzle using the methods described in Section 3.1.1.

Three bubbles were emitted for each set of rods. An average bubble volume for each rod diameter is reported in Results. Table 1: Metal rods used for varying rod diameter experiment. Measured diameters are reported. is a list of common objects and their diameters that were used for this test.

Table 1: Metal rods used for varying rod diameter experiment. Measured diameters are reported.

Object	Diameter (mm)
Syringe tip	0.25
Staple	0.48
Sewing needle	0.53
Pin	0.59
Sewing needle	0.69
Small paperclip	0.80
Sewing needle	0.88
Large paperclip	1.15
Sewing needle	1.22

3.1.3 Effect of air injection rate

3.1.3.1 Effect of non-continuous flow

Initial tests were run with a 10 microliter syringe, to an accuracy of 0.1 microliter. Air was injected through the side of the nozzle directly from the 10-microliter syringe. After emptying the syringe, it was removed, refilled, and reinserted into the nozzle. The process was repeated until the bubble detached from the nozzle.

There were two advantages offered by the 10 microliter syringe over something larger. Volume measurements were more precise and air injection rate was kept low and nearly constant. The effect of airflow rate on bubble volume will be discussed in the Results section.

3.1.3.2 Effect of non-continuous flow

A larger syringe offered a different advantage. A 100 microliter syringe held more air than was necessary to inject into the nozzle to create one bubble. With the 10 microliter syringe, the

syringe had to be removed 10 microliters of air were inserted into the nozzle. To reach typical bubble volume for the general experiment set up (between 60 and 70 microliters), many reinsertions were required to reach pinch off. Without halting at every interval of 10 microliters, constant air flow rates were recorded. Measurements were only accurate to 1 microliter.

In order to ensure constant air flow rate, the syringe was inserted into a thin rubber hose and sealed. The hose inserted into the bottom of the nozzle and sealed with putty to the bottom of the tank. The hose was 5 cm long and 0.50 mm in diameter.

A close to constant injection rate was achieved by adding weights to the top of the syringe and allowing them to slowly push air into the hose. Weight was increased to the point of the system still being stable. Below is a picture of the entire set up, as well as a close up of the hose attached to the nozzle.

(a) (b)
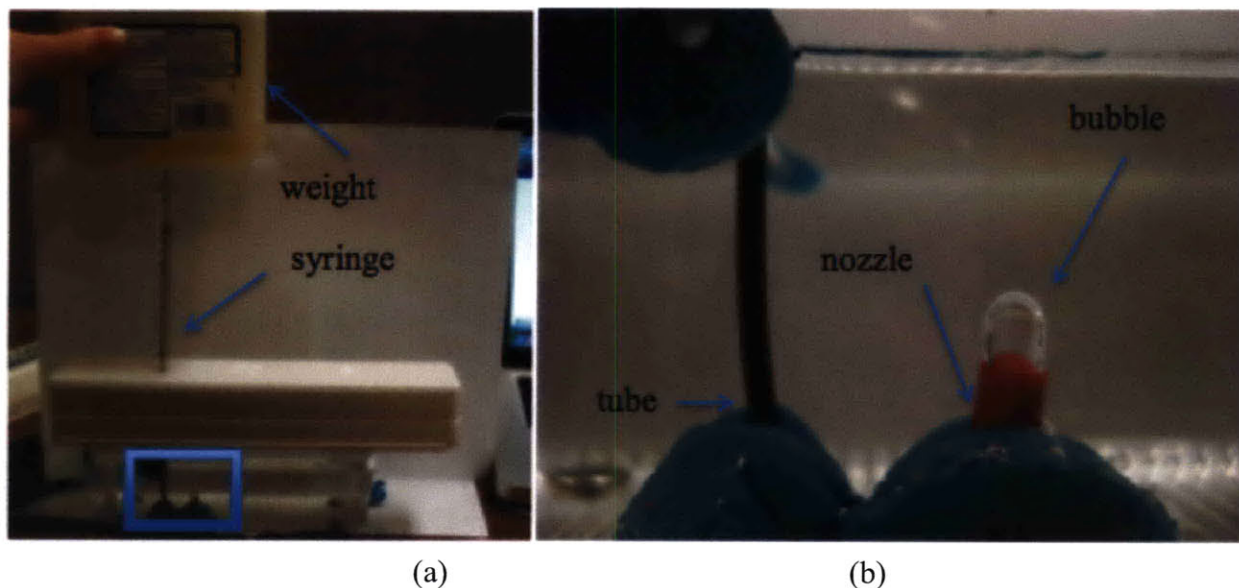
Figure 11: Continuous air flow experimental set up, (a) location of weight application (base of the syringe) and (b) hose connecting syringe to the bottom of the nozzle. Putty affixes system to the tank.

Air flow rate was calculated by dividing the total starting volume in the syringe by the measured time to empty the syringe. Total time to empty the syringe was measured and recorded. In initial tests, a full screen stopwatch was activated behind the tank. Time recording was halted when the syringe emptied. Video was taken of each data collection. Elapsed time was visible in the video frame and accurate to the thousandth of a second. Air injection commenced into the nozzle at the same time the stopwatch was activated, so time to bubble detachment was easily measured through inspection of the video. The time to create a bubble was then multiplied by the rate of air injection to determine the bubble volume.

The initial round of tests produced variability at high flow rates. Air injected at rates above 15 microliters per second were greatly affected by slight variation in time data collection. If the stopwatch was not activated exactly at the moment that air injection was started and not stopped at the moment air injection ceased, data showed discrepancies. For a high injection rate, a small time lag will have a greater effect than at a lower injection rate.

The set up was modified so that the clock was running continuously and no coordination was required between air injection and starting or stopping of time collection. The bubble, syringe end, and time reading were all captured within the same frame of video collection. Analysis was performed after data collection to determine the time to emit the bubble and the rate of air injection.

3.1.4 Water surface tension

Surface of tension of the fluid in the tank was varied between 45 and 72 mN/m. First, bubbles were emitted into the tank without the presence of parallel rods above the nozzle. Next bubbles were emitted between rods spaced 4.3 mm apart. Multiple measurements were taken for each of these two setups at each different surface tension. Averaged bubble volumes for each of the two cases were compared to make a dimensionless volume for each alcohol concentration.

Surface tension of the fluid was varied through the addition of small volumes of ethyl alcohol. Ethyl alcohol concentration was varied between 0 and 20% by volume. Data collection was stopped at 20% ethyl alcohol. Bubbles were of so low diameter at 20% alcohol solution that they did not stick to the rods. More importantly, larger percentage values compromised the experimental set up. With much lower surface tension at 25% alcohol by volume, air was not retained uniformly in the underwater nozzle. Surface tension was not high enough to prevent wetting of the interior of the nozzle.

Bubble volume was recorded at each differing alcohol concentration. Results are reported later. Using published surface tension data, based on differing ethyl alcohol concentrations in water, bubble volume was then related to surface tension.

The data below was used for the dependence on surface tension on ethyl alcohol concentration.
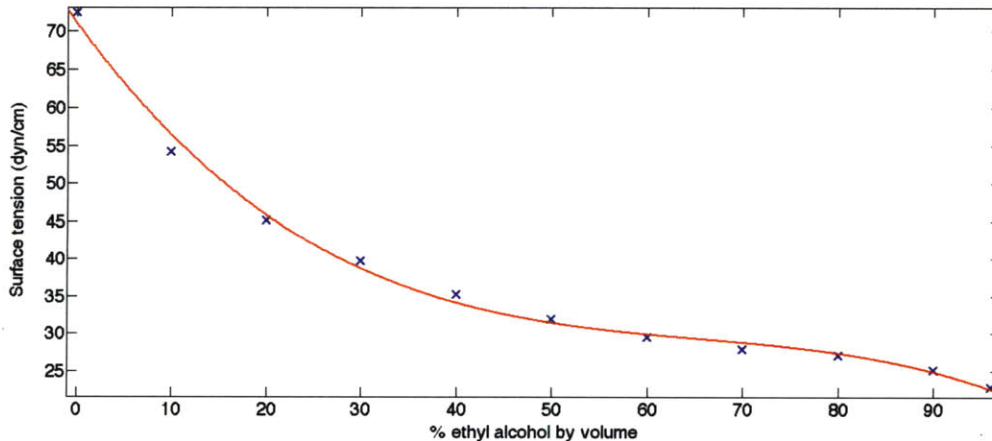
Figure 12: Previously obtained data for the relationship between surface tension and the percentage of ethyl alcohol in water (Kiriyanenko 1968)

3.1.5 Effect of water height

Tests were performed to determine whether water height above the nozzle affects bubble volume. Bubbles were emitted under water heights of 2 cm and 4 cm. All other conditions were

held constant. Water was at room temperature (between 20 and 24 degrees Celsius), there were no rods above the nozzles, and nothing was added to the fluid to alter surface tension.

3.1.6 Effect of nozzle diameter

Nozzle diameter was varied by constructing nozzles out of various drinking straws. Nozzles were attached with airtight seals to the bottom of the tank and emitted bubble volume and shape was observed.

3.1.7 Effect of angle of bubble emission

Angle of the nozzle from the horizontal was varied. The test was performed to determine whether the angle of the nozzle had an effect on the bubble volume. The nozzle was attached to a plastic protractor and submerged in the tank. Angle of the nozzle relative to horizontal was varied between 0 and 90 degrees, with bubble volume measured at increments of ten degrees.

3.2 Bubble Capture Device

3.2.1 General experimental set up

Drawing from the observations made in the nozzle experiments, new experimental set up was designed. In this section, the bubble capture device is described, along with the experiments used to study bubble behavior in the device.

A device was built for passive capture of bubbles. When the device is submerged into the tank of water, a bubble forms within the frame. The purpose of the device is to observe how changing environmental parameters affected the bubble volume captured in a fixed geometry device. The frame was made of staples, bent to shape using needle nosed pliers. Measurements were taken to assure equal angles of bending between each rod in the device. In Figure 13, a photograph of the device is shown with critical dimension. Also visible in the picture is a captured bubble.
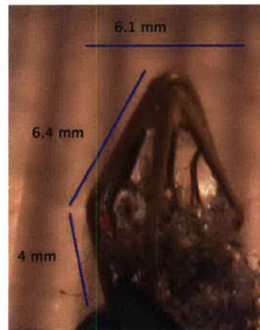
Figure 13: Bubble capture device with critical dimensions. The six rods are each half a staple, hydrophobically coated fabric is used as the central surface covering.

Rods were of diameter 0.48 mm. Staples were unfolded at the sides and folded down the middle to create each set of rods. A strip of fabric was coated with hydrophobic spray, and is from now on referred to as the hydrophobic sponge. The sponge between the rods was 4 mm wide. As discussed later in the results, the sponge had an important role in bubble formation.

As the device is submerged, the rods and sponge attract air, preventing wetting. Below is a two dimensional progression of the shape of the air-interface between the rods as the device is submerged.
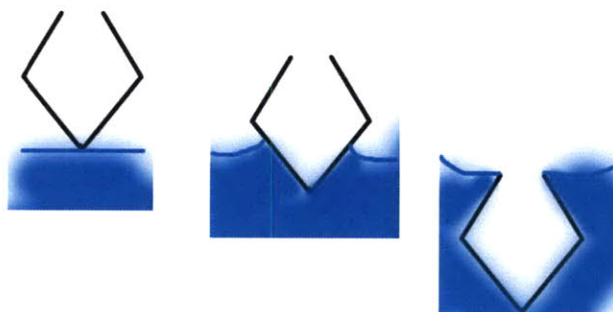
Figure 14: Two dimensional progression of the bubble capture device as it is submerged into water.

The following progression shows how a bubble forms as the device is slowly submerged into the water.
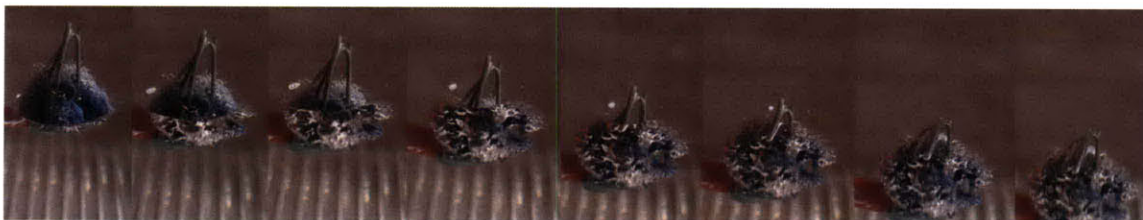
Figure 15: Progression of the bubble capture device as it is submerged in the water, capturing a bubble. In the first three pictures, the fluid line is visible on the side of the hydrophobic sponge. In the fourth picture, the sponge is completely submerged. In the fifth, sixth, and seventh pictures the device becomes increasingly submerged, until the eighth picture, where the device is completely submerged. The bubble inside the device is visible between the rods.

Preliminary tests were run to establish conditions for the following experiments. These tests involved the development of the device.

The number of rods forming the frame of the device was increased until a bubble was captured passively. Six rods, made of three staples, were used in the final design. Rods were spaced at equal angles from each other, meeting at the top and at the bottom of the device. Rods were coated in hydrophobic spray. The can was held 10 – 12 inches away and sprayed for 20 seconds on both sides of the rod.

Extensive testing went into developing a device with only two rods to more closely mimic the spider. The device did not passively capture air bubbles. The water spider does not capture bubbles simply with two legs, it instead uses another set of legs in a swift cutting motion to detach the bubble from surface. Methods of cutting the bubble off from the interface between air and fluid were experimented with. Additional rods were first used, and then a flat razor. The design was abandoned after many trials with a consistent absence of bubble formation.

The rods are bent to form a 120 degree angle at their centers. The rods were sprayed with a hydrophobic coating. At the base of the rods is a strip of fabric coated in hydrophobic spray. The fibers projecting from the surface have a maximum of 3 mm length. Initially, tests were run

in distilled water for comparison against tap water. Differences in bubble volume captured were negligible. To save cost and time, tap water was used for testing.

A simple actuating mechanism was built to lower the device into the tank at constant speed. The majority of tests were performed at low submersion speeds by hand, as results from the speed submersion test showed that at very low speeds, the effects slight differences in speed are negligible on resulting bubble volume.

Bubble volume was measured by emptying the air from within the device while it is still submerged. A 100 microliter syringe was used to empty the bubble. There were two indicators that the bubble had been completely removed. First, visual observation was used. A more reliable method was when the bubble was emptied, the syringe began to fill with water. Water and air are easily differentiable in the syringe, so the volume of water taken up by the syringe was be subtracted from the total volume taken by the syringe to obtain the air removed from the device.

Observations of bubble shape were taken visually. A standard digital camera was used to capture images of static bubbles and of the process of bubble capture. The series of experiments are outlined in the following subsections. Each addresses a scientific question identified in the introduction.

3.2.2 Effect of fluid surface tension

Surface tension forces kept the bubble from escaping through the framework of the device. Similarly to the previous experiment, ethyl alcohol was used to alter the surface tension of water. The relationship between surface tension and captured bubble volume was observed and data was recorded.

In order to measure the effect of changing surface tension on bubble volume, all parameters of the experiment were fixed except for surface tension of the fluid. Surface tension of the fluid was altered by adding increasing concentrations of ethyl alcohol. A 70% ethyl alcohol solution was used to alter the surface tension of the fluid. Alcohol concentration was varied between 0% and 10% ethyl alcohol by volume. Experiments were ceased above 10% alcohol concentration because there was no observed bubble formation.

Tap water from the same faucet was used for all runs of this experiment. There was therefore no assumed difference between batches of water used for each of the surface tension trials. Water temperature varied between 20 and 24 degrees Celsius over the course of all trials, not a large enough margin to alter the surface tension enough to skew the results.

3.2.3 Effect of speed of submersion

Experimenting with the bubble capture device by hand, it was clear that submerging the device at relatively high speeds reduced the volume of the bubble captured. A quantitative experiment was developed to determine the behavior of bubble capture at different speeds.

The speed at which the device was brought below the surface of the water was varied to observe the affect on bubble volume. A simple mechanism was used to achieve speed variation. Speed was kept constant through the course of a submersion process. This was achieved by developing a constant speed device. As shown in the figure below, a DC motor was used to wind up and release the device into the water.
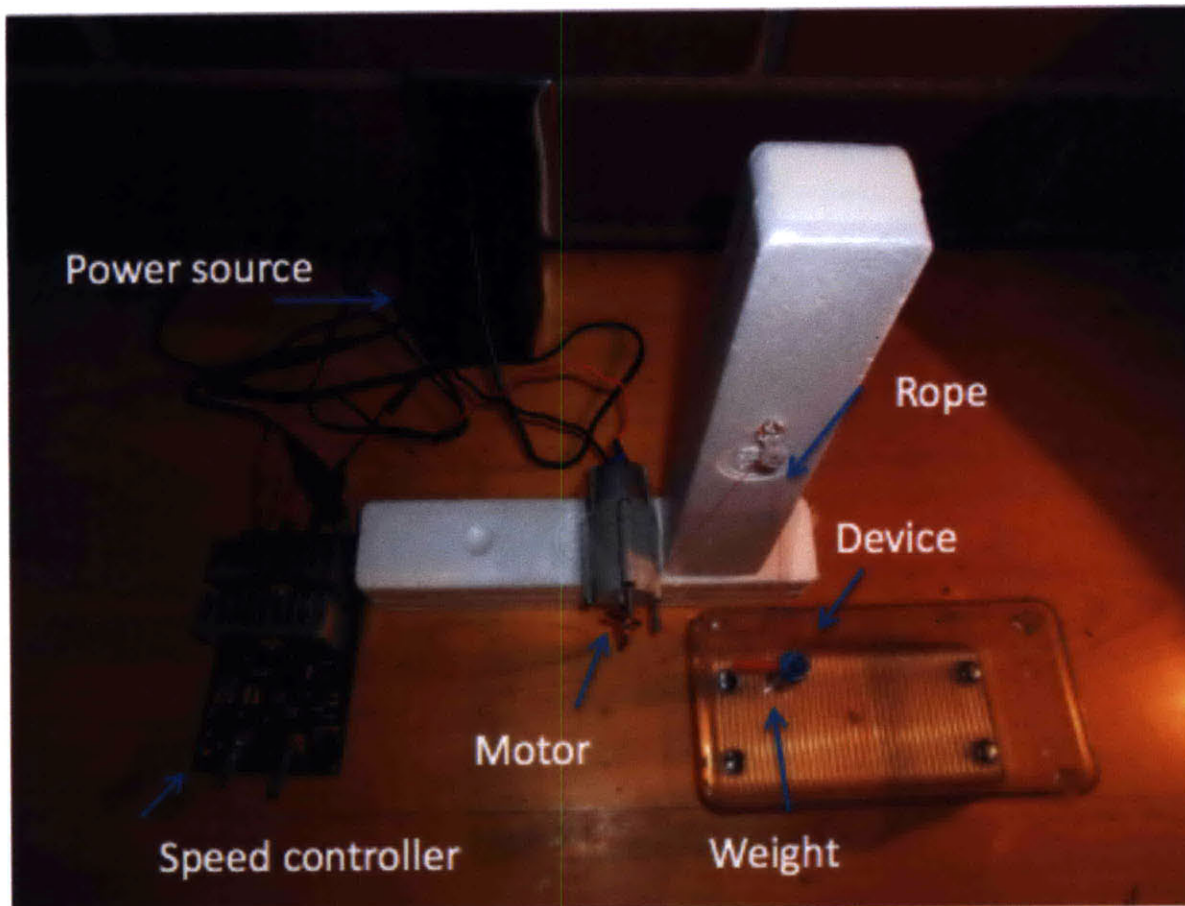
Figure 16: Photo of constant submersion speed mechanism for the bubble capture device.

The mechanism was built from a DC motor, speed controller, plastic, tape, and string. The purpose of this initial mechanism was to determine whether submersion speed had a significant effect on bubble volume. Submersion speeds were varied between 0 and 4.5 cm/s. The speed controller did not explicitly give a reading of output rpm. It was used for easy variance of speed and to keep constant speed for the course of a trial. Measurements of the distance traveled by the device were recorded, as well as total time of travel.

As discussed in Results, below a certain threshold speed, volume remained at the maximum, so a more permanent mechanism was not developed. Subsequent tests were run by hand, well below the threshold speed.

3.2.4 Qualitative Observations

The hydrophobicity of the device is important to the bubble capture capacity of the device. The details of this relationship are difficult to quantify, so basic comparisons were made. A series of tests were run to make qualitative observations regarding parameters of the device. Hydrophobicity of the device will be altered over the range of no hydrophobic enhancements to surface treatments and textures. Parameters were altered to observe differences between the chosen set up and possible other designs. The following conditions were examined:

1. Hydrophobic coating on rods
2. Hydrophobic sponge
3. Number of rods

The first question addressed whether or not adding a hydrophobic coating to the rods enhanced the bubble capture ability of the device. Hydrophobic coating was sprayed on one device, while the other was left clean. The same coating procedures as detailed in the coating of the parallel rods in the underwater nozzle experiment were followed. The experiment was performed using the six rod design for both the coated and uncoated case. Both were submerged in the water at a rate of approximately 1 mm/s. All other conditions were held constant between the two cases. Behavior of the liquid and fluid in the device was examined. Temperature of the fluid was in the range of 20 to 24 degrees Celsius.

The second condition regards the hydrophobic sponge between the rods at the base of the device. Made of common sweatshirt material, with the soft side facing out, the fabric was coated with the same hydrophobic spray used on the rods. Strips of the fabric were cut 4 mm wide and threaded between the rods of the device. The fabric completely covered the base of the device. Fibers extended a maximum of 3 mm out from the fabric when held straight. When observed in their natural curled state, the fiber profile only extended 1 mm from the fabric.

The fabric was used to mimic the hairy abdomen of the spider. The spider's abdomen projects between the two back legs, seeming to enhance the bubble capture capacity of the spider. Two experiments evaluated the importance of having a hydrophobic hairy surface in addition to the legs. The first experiment addressed the question of whether or not the hydrophobic sponge was necessary for bubble formation. One device with the sponge and one without were submerged in water, all other conditions held constant. The second experiment compared a standard sized sponge to one twice the size.

The third condition of importance is the number of rods used to form the device. The water spider uses two legs to hold the bubble and two more legs to separate the bubble from the surface. Because this device is a passive device, more than two legs are necessary to capture the bubble and bring it underwater. Devices with 2, 3, 4, 5, and 6 rods were submerged to observe the differences in fluid air behavior between the rods and to evaluate how many rods are necessary for bubble formation.

Table 3 in Results shows photographs of each of the discussed cases, along with written observations and information about whether or not bubble formation occurred.

4   Results and Discussion

4.1   Underwater nozzle experiments

4.1.1   Effect of side rods

Parallel metal rods placed around the nozzle affected the bubble volume emitted at pinch off. Volume of the bubble depended on spacing of the rods.

4.1.1.1   Effect of side rod spacing

The results of side rod spacing experiments are shown in Figure 17. Nozzle diameter, materials, water temperature, surface tension, and airflow rate were held constant throughout this set of tests.

Figure 17: Dimensionless bubble volume v/v_0 is plotted against dimensionless rod spacing d/D. The constant $v_0 = 67.2$ is the average measured bubble volume emitted from a nozzle not in the presence of parallel rods. Reference length $D = 4.3$ is the inner diameter of the nozzle. Bubble volume v and rod spacing d vary. Temperature of the fluid is between 20 and 24 °C. Bubbles at maximum, right before pinch off are shown in the progression above the graph.

Dimensionless volume is compared to dimensionless diameter in Figure 17. Dimensionless volume was calculated by dividing the measured volume v by a standard volume v_0. The standard volume in the plot above was obtained from the emission of a bubble through a nozzle without surrounding rods, all other conditions held constant with the rest of the experiment. Ten measurements were taken and averaged to obtain standard volume $v_0 = 67.2$ microliters for the rod spacing experiment. Using the ten measurements, error in bubble volume measurements at pinch off was calculated to be 0.89 microliters. This error is approximately 1.3% of the mean.

To calculate dimensionless length, space between the rods d, was divided by the constant nozzle diameter D. For all nozzle experiments, $D = 4.3$ mm. Rod spacing d varied between 0 and 5 mm.

As can be seen in Figure 17, there were three critical points marking changes in the shape of the graph. Below the first critical rod spacing, bubble volume was smaller than that emitted from a nozzle into free water. This occurred when the ratio $d/D = 0.8$. At this point, bubble volume was equal to that of a bubble emitted into free water with no nozzles. Rod spacing was 80% of the inner diameter of the nozzle. While the bubble was not as wide as a bubble emitted into free water, the rods extended the length of the bubble, balancing out to the same volume as would be emitted into free water.

Above the first critical value, bubble volume increased above the volume that was emitted into free water. Bubble volume increased until the second critical point. At this spacing, bubble volume was maximized. The distance ratio d/D = 1 at maximum bubble volume. Maximum bubble volume was 81 microliters. Bubble volume was 15% greater than the standard case, bubbles emitted through a nozzle with no rods.

At greater spacing, bubble volume decreased, until the third critical point. After the third critical point, bubble volume remained constant. The critical point where bubble volume stopped changing was at rod spacing of 4.9 mm, or $d/D = 1.2$. Above $d/D = 1.2$, bubbles did not attach to the rods, so bubble formation was identical to the case without rods. For this reason, the ratio v/v_0 was 1. From this point forward, the bubble volume observed between rods was the same as bubble volume without rods, so the volume ratio was 1.

Minimum bubble volume occurred when the rods were touching, or at 0 spacing. Bubble volume was 30% lower than the standard case. When rods were spaced close together, bubble volume at pinch off was decreased from the case with no rods because the rods interfered with bubble formation.

The results of the rod spacing test gave insight into the spacing between the spider's back legs. The legs are spaced so as to increase the bubble volume above what would be captured around the abdomen. The water spider's abdomen is hydrophobic. When submerged, the abdomen passively retains a thin layer of air, called a plastron. As discussed in Section 2.1.3, it has been proven that the water spider breathes through this passively maintained air layer.

While it is essential to the water spider's survival that it can passively maintain this thin air layer, it is also important that the spider be able to capture larger air bubbles. If the spider were to rely only on its plastron for breathing, it would have to continually have to surface and replenish the oxygen in the plastron. Female water spiders especially must stay in one place for a longer period of time, when they are reproducing. They must create an underwater habitat in which there is enough air to breathe for up to a month at a time. The mechanism by which they capture large bubbles is critical to survival.

The rod spacing experiments show that the evolutionary feature of longer back legs allows the water spider to capture the necessary bubble of air, not making an excessive number of energetically taxing trips to the surface to replenish the oxygen in its habitat.

4.1.1.2 Effect of rod texture

Bristled rods replacing the smooth hydrophobic rods did not increase the maximum bubble volume emitted from the nozzle. A greater bubble volume was expected with the use of bristled

rods, and even larger for hydrophobically coated bristled rods. Neither increased the volume. Figure 18 shows the dimensionless bubble volume as a function of dimensionless rod spacing.
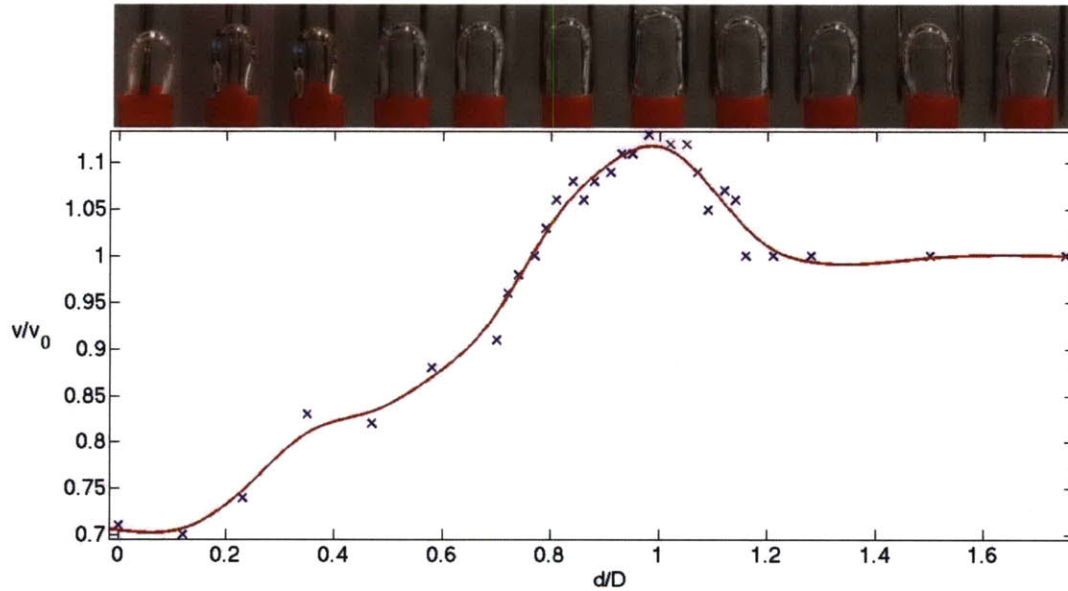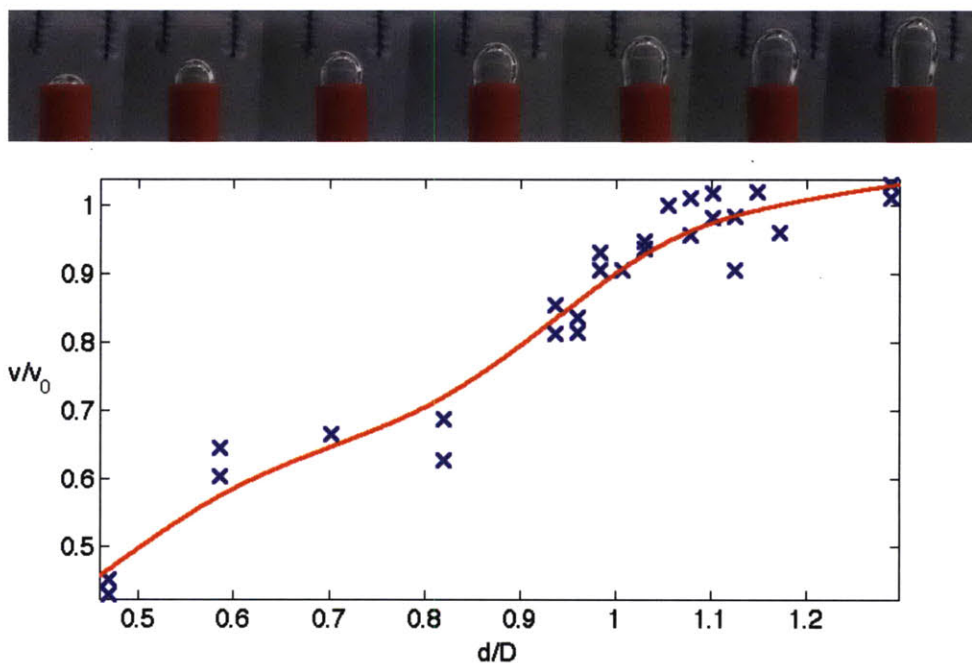

Figure 18: Dimensionless bubble volume v/v_0 is plotted against dimensionless rod spacing d/D. The constant $v_0 = 67.2$ microliters is the average measured bubble volume emitted from a nozzle not in the presence of parallel rods. Reference length $D = 4.3$ mm is the inner diameter of the nozzle. Bubble volume v and rod spacing d vary. Rods are covered with plastic bristles. Temperature of the fluid is between 20 and 24 °C.

Uncoated brushes did not increase the volume of air that could be trapped as was originally expected. The bristles interfered with bubble formation rather instead of enhancing it. When the rods were spaced equally with the outer diameter of the nozzle, the bristles overlapped into the nozzle area. This hampered the development of bubbles and resulted in lower than maximum volume. In the case of this experiment, maximum volume was obtained when the bubble formed without the interference of the bristles.

Decreasing the distance between the rods from the width of the nozzle by 60%, bubble volume decreased 60%. The relationship, however, does not appear linear.

It was hypothesized that textured rods would increase the volume of the bubble before pinch off. The bristled rods used for this experiment did not increase bubble volume, rods with different texturing could have the opposite effect. Additional exploration into textured rods could be performed to gain more insight into this problem. The scale of roughness might be much smaller. Roughness could be etched into the surface of the rods.

This experiment does provide any insight into the characteristics of the water spider. While the spider's legs were used as inspiration for the bristled rods, the bristles are not on the same length scale as the hairs on the spider's legs. Much more investigation could go into better mimicking the surface of the water spider's legs.

4.1.1.3 Effect of rod diameter

In the first round of testing, diameter of the parallel rods was first doubled, then raised by a whole order of magnitude. Results of this test were not of significance. Doubling the diameter yielded similar bubble volume results. Increasing the rod diameter by a factor of nearly 10 showed a decrease in bubble volume. At this diameter, the bubble only attached to one post. This may explain the fact that the observed bubbles were slightly lower volume for the much thicker posts. In previous experiments, when the bubble only attached to one rod, bubble volume was lower than when it attached to both rods. The results are graphed below in Figure 19.
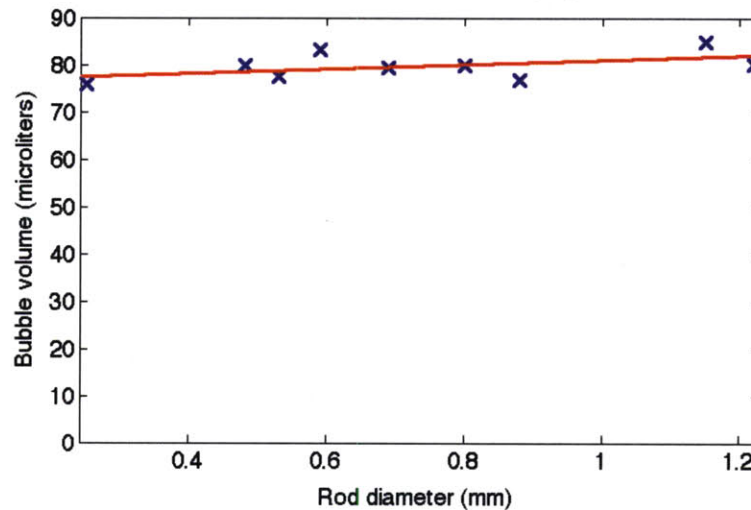
Figure 19: Bubble volume (microliters) plotted against rod diameter (mm). Temperature of the fluid is between 20 and 24 °C.

From the graph, there is no apparent trend or relationship concerning bubble volume and rod diameter. Data was not presented in a dimensionless format because of the lack of trend. Rod diameter did not affect the bubble volume. It is apparent from Figure 19 that bubble volume remains relatively constant while rod diameter changes.

The purpose of the experiment was to test whether thickness of the spider's legs affects bubble volume. It is expected that in the case of the water spider, given the same surface features, increase the diameter of the legs would increase the captured bubble volume. An increased diameter would correspond to a larger surface area, with more opportunity for the legs to grab more air.

Further experimentation would have be more precise. Slight differences may be outside the scope of the current experimental procedures. Fractional millimeter changes in the diameter of the rods could correspond to fractional microliter changes in bubble volume. For the current study, rod diameter can be eliminated as a significant parameter in bubble volume.

4.1.2 Effect of air injection rate

As shown in Figure 20, as air injection rate increases, bubble volume decreases. At an injection rate of 5 microliters per second, bubble volume is at the maximum.
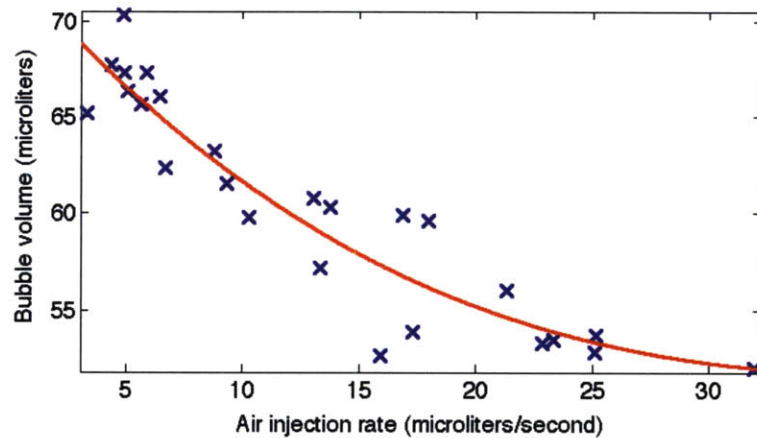
Figure 20: Bubble volume (microliters) plotted against rate of air injection (microliters/second) into the underwater nozzle. Temperature of the fluid is between 20 and 24 °C.

The air injection rate experiment was performed in the pursuit of decreasing the variability in bubble volume measurements. Constant injection rates were used, but observed variability was high. Over an increase of 500% in injection rate (from 5 to 25 microliters per second), bubble volume decreased by approximately 23 percent. As can be seen in the graph, this is outside the realm of variability, so increasing the injection rate does decrease the bubble volume.

Bubble volumes at high flow rates had high variability. This variability is due to the limitations of the instrumentation. At an injection rate of approximately 15 microliters per second, variability jumps. A clear correlation is visible for injection rates below 15 microliters/second. Data collection was discontinued as a higher variability at higher flow rates was observed. As stated, the aim of this experiment was to decrease variability at lower rates, but this did not happen.

As a result of this air injection experiment, constant flow rate of air into the nozzle is not deemed important. It is more important to keep the injection rate below a certain threshold value. The threshold value 5 microliters per second. At air injection rates below this value, speed variability has no effect on bubble volume.

Flow rate can be ruled out as a parameter in the original rod and bubble volume experiment. Flow rates used in those experiments were within the range of the slowest rates recorded in this experiment. Injecting 80 microliters at 4 seconds per 10 microliters, multiplies to 32 seconds per bubble. This is roughly the value of the slowest injection rates with the larger syringe.

4.1.3 Effect of fluid surface tension

Inspecting Figure 21, the bubble volume ratio decreases linearly with increasing ethyl alcohol percentage.
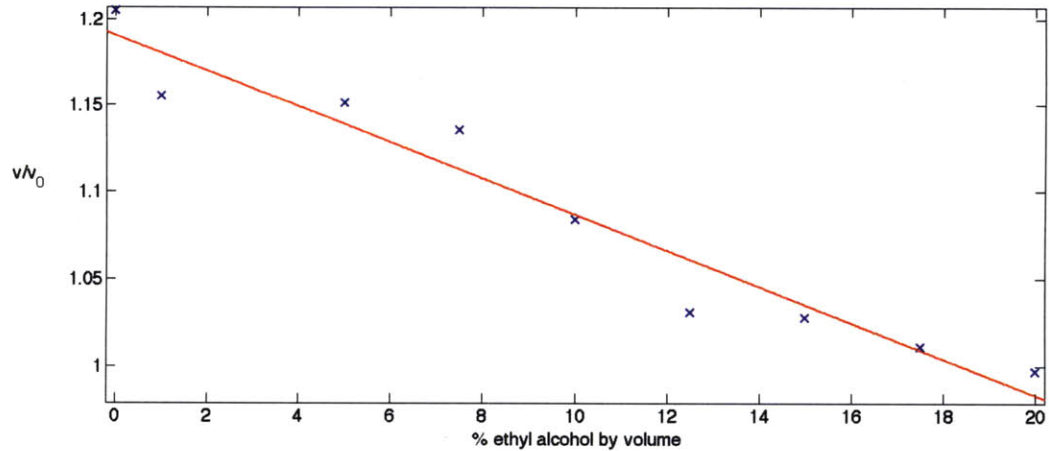
Figure 21: Dimensionless bubble volume v/v_0 is plotted against percentage of ethyl alcohol in the fluid by volume, temperature of the fluid is between 20 and 24 °C. Bubble volume data is non dimensionalized against minimum bubble volume $v_0 = 56$ microliters.

This observation is logical upon comparison to the plot of surface tension versus ethyl alcohol concentration. The curve can be decoupled to two linear portions on either side of 30% alcohol concentration. For the current experimental set up, only water with a 20% concentration of ethyl alcohol by volume was used. Values above this threshold were increasingly difficult to measure consistent results. As surface tension drops below 20 mN/m for water with 30% ethyl alcohol by volume, air cannot be maintained throughout the underwater nozzle. It is essential to the experimental set up that surface tension maintains air in the nozzle otherwise it is impossible to emit uniform bubbles.

An aggregate plot was constructed to show how bubble shape visually corresponds to measurements. The results of varying alcohol concentration are shown in Figure 22. High surface tension corresponds to low alcohol concentration. As explained previously, measurements were only taken up to a maximum of 20% alcohol solution. From the figure, it is apparent that as surface tension increases, so does bubble volume.
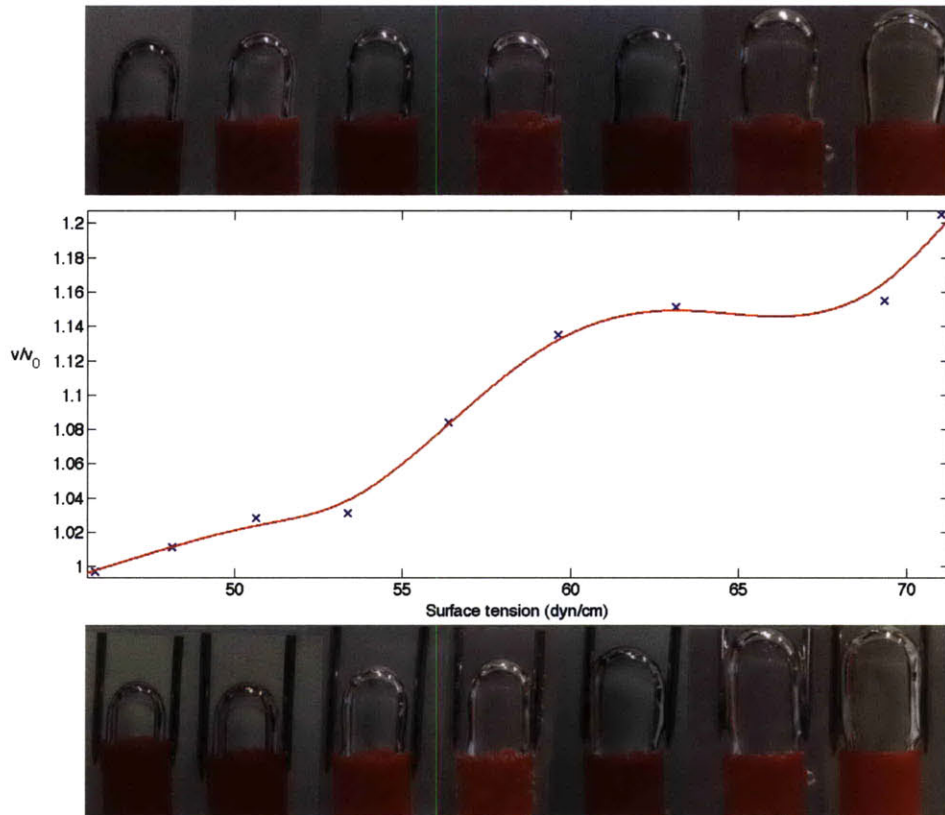
Figure 22: Dimensionless bubble volume v/v_0 is plotted against surface tension of the fluid, temperature of the fluid is between 20 and 24 ˚C. Standard bubble volume, taken when the bubble is emitted into open water, is 67.2 microliters. Volume data is for bubble emitted between parallel rods. Top progression shows bubble formation from nozzle into open water, bottom progression shows bubble formation from nozzle between rods.

The water spider would be drastically affected by drop a small drop in surface tension. Based on the shape of the graph, bubble volume drops most sharply when surface tension is decreased just below that of pure water.

4.1.4 Effect of water height above the nozzle

There was no measurable difference in bubble volume when water height above the nozzle was doubled. This may be because the standard water height was only 2 cm so doubling it should have no measurable effect on pressure at the nozzle. For the current study, which involves gathering bubbles from the water surface, it is not necessary to examine what happens at greater depths. This may become pertinent information as the idea progresses and the bubble is retained at greater depths.

Water height did not change the volume of bubble emitted from the nozzle. With the current experimental set up, with 0.1 microliter precision, small changes in water height may be outside the scope of measurement. Water height could be greatly increased for a more extreme case, but

that would require a different experiment set up. All of the experiments in the current study were performed in the same shallow dish.

There is no comprehensive set of data of typical depths at which the water spider builds its habitat.

4.1.5 Effect of nozzle diameter

The effect of nozzle diameter on bubble volume was briefly explored. Nozzles of three diameters were tested. The very basic trend shows that the nozzle size used for the rest of testing is in the realm of the geometry for optimal bubble size. The purpose of this test was to confirm that the nozzle being used in the experiments was of suitable geometry given the properties of the fluid. After testing nozzles of other sizes, it was clear that the nozzle in use gave the clearest picture of the bubble as it grew and all the way to pinch off.

4.1.6 Effect of angle of bubble emission

Again, photographs of the bubbles are aligned with corresponding data points. The vertical axis is again non-dimensional volume, with the v_0 term corresponding to bubble volume at perpendicular and the v term representing the measurement taken at that angle. There is a steady rise in bubble volume as angle increase to 60 degrees. After this point, the curve changes shape, having a much slower rate of increase at it stabilizes to unity.
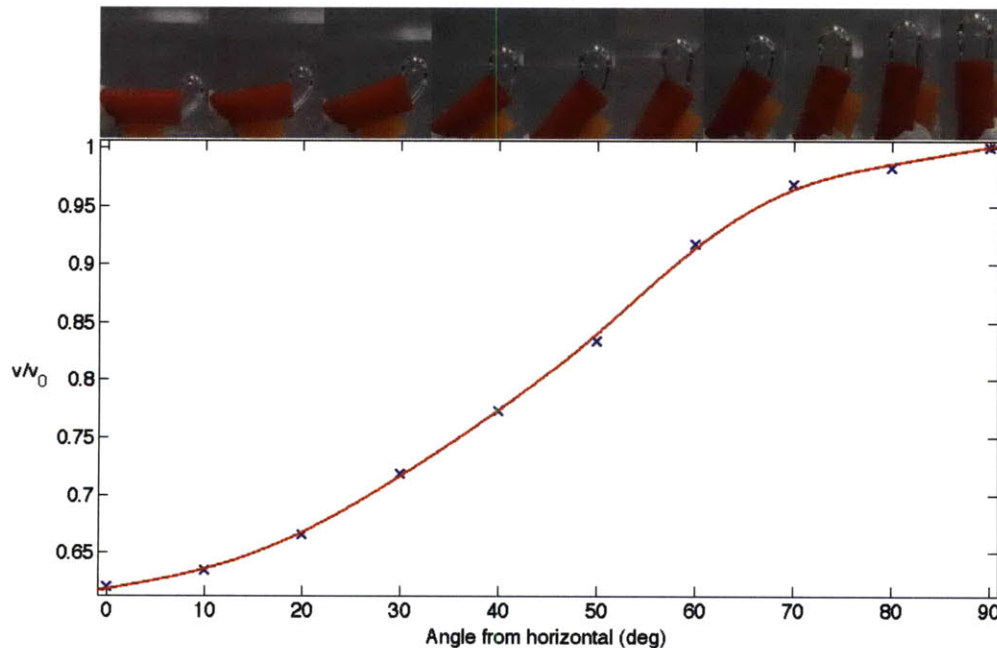
Figure 23: Dimensionless bubble volume v/v_0 is plotted against angle the nozzle makes with the horizontal, temperature of the fluid is between 20 and 24 °C. Standard bubble volume, taken when the nozzle is perpendicular to the tank, is 67.2 microliters.

When the nozzle was parallel to the bottom of the tank, the bubble volume was 60% the size of the bubble emitted when the nozzle was perfectly perpendicular. This experiment showed that

41

perpendicular alignment is ideal for maximum bubble volume. The perpendicular nozzle was already a standard condition for testing.

Angle of bubble emission, height of water above the nozzle, and air injection rate were eliminated as critical parameters. While angle of emission and airflow rate can affect bubble volume, they are also simple to hold constant and it is practical to do so. For air injection rate at low levels, there is negligible effect on bubble formation. Experiments were run well below the cutoff, between 2 and 4 microliters per second. The only experiment with higher flow rates was the one in which flow rates were varied.

Surface tension of the water, as well as the diameter of the nozzle and spacing between the rods had the greatest effect on bubble volume when small changes were made in each of the parameters. The goal of the experiment, to determine whether parallel rods increase the volume of the bubble was achieved.

Finer instrumentation would be necessary to get more precise results in all tests. A larger syringe would be ideal. The reason for this is the variability in the flow rate inherent to the syringe. With a constant force applied to the syringe, the flow rate naturally varies with the friction inside of the syringe.

For future work, bubble formation can continue to be studied. The effects of additional surfactants, as well as acoustic pollution could be studied. Another direction would be to apply the study to coating an object in bubbles. Emitting air through tiny nozzles all over a surface could be an active mechanism for attaining an underwater air coating. With a better understanding of the effect of parallel rods on bubble dynamics and formation, there is much more that can be done in the mimicry of the water spider.

4.2 Bubble Capture Device

4.2.1 Effect of fluid surface Tension

Figure 24 shows the results of surface tension experiments with the bubble capture device. The plot is of an aggregate set of data, results were repeated and averaged over three separate experiments with the device described above. Dimensionless bubble volume is plotted as a function of the percentage of ethyl alcohol in the solution. The rest of the solution was tap water.
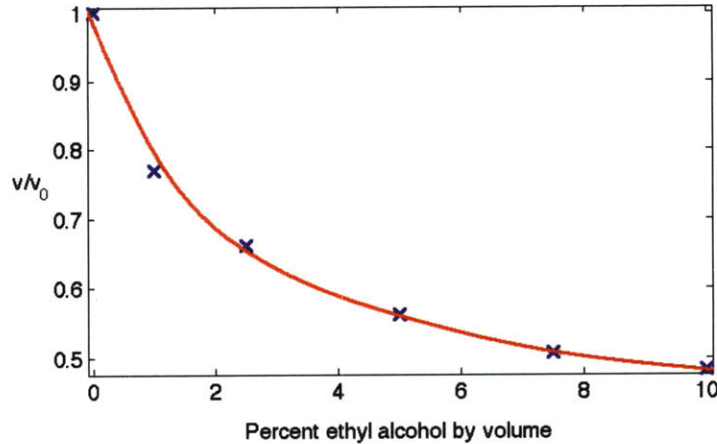
Figure 24: Dimensionless bubble volume, v/v_0, plotted as a function of percentage of ethyl alcohol in water solution, where bubble volume at 0% alcohol $v_0 = 59$ microliters is used as the standard point by which the rest of the data is non dimensionalized. Measurements taken in fluid of temperature between 20 and 24 degrees Celsius.

Dimensionless bubble volume was calculated using $v_0 = 59$ microliters as the reference value. The value v_0 was the average bubble volume captured by the device in 0% alcohol solution. Ethyl alcohol was added to create increments of 2.5% alcohol percentage, plus measurements at 1% alcohol. Ethyl alcohol percentage was varied between 0 and 10%. Alcohol tests were all performed at low submersion speeds, on the order of 1 mm/s. This falls in the region of maximum bubble volume found in the following section.

Measurements were ceased at 10% ethyl alcohol concentration because bubbles stopped forming. Based on previous literature, 10% alcohol concentration corresponds to a surface tension of 54.2 dynes per centimeter. Water with no alcohol added has a surface tension of 72.4 dynes per centimeter. Therefore, bubble volume decreased by approximately 50%, over the range of a 25% decrease in surface tension. Bubble volume decreased rapidly between 0 and 2.5% ethyl alcohol concentration. After 2.5% alcohol, bubble volume still decreased but at a slower rate.

The only difference between expected and measured results is occurs at very low concentrations of ethyl alcohol. It was expected that small concentrations of ethyl alcohol would not greatly affect the bubble volume. In experimentation, it was clear that any small addition of alcohol drastically altered the volume of the bubble that could be captured.

Figure 24 can be compared to observed effects of surface tension in the underwater nozzle experiments. Here, a similar trend in data was observed, although over a larger range of surface tension. Surface tension was decreased by 36% in the nozzle experiment, but bubble volume only decreased by 17% over the same range. While the ranges were different, the same general trend was followed. Differences can be attributed to the fact that the systems differ widely in how bubbles are formed. Behavior is different across the different bubble formation methods.

In the nozzle surface tension experiment, bubbles ceased to form reliably from the nozzle at 20% ethyl alcohol concentration in the water. In the corresponding bubble capture device experiment, bubbles did not form at 10% ethyl alcohol concentration. The difference could be

43

due to the way the bubble interacts with each set up. For the nozzle, there is a larger volume of air stored in the nozzle. The bubble device is capturing the bubble, separating it completely from the surface, and must be maintained in a given volume. As surface tension decreases, characteristic bubble size will decrease, meaning that a smaller bubble would not stay trapped in a device of fixed geometry.

The water spider would be drastically affected by a decrease in surface tension. It would not be able to capture bubbles of the necessary volume. It is possible that the volume of the plastron would also reduce to a dangerous value. More investigation could be performed to investigate the effects a drop in surface tension would have on air bubbles the size of the plastron.

The results of the surface tension experiment are important when considering scaling up the size of the device for real applications. If the device were to be scaled up, the role of surface tension would be very different. Surface tension would have less of an effect, meaning that the effective surface tension would be much lower, all other conditions held constant. When scaling up the current device, bubble volume relative to the device will decrease unless other parameters are altered. Surface area of the rods could be increased, additional hydrophobic surface treatments could also be used.

4.2.2 Effect of speed of device submersion

As described in Methods, a mechanism was built to achieve constant speed of submersion of the bubble capture device. Speed of submersion was varied in a range of 1.6 to 45 mm/s for the device in tap water. In Figure 25, dimensionless bubble volume is plotted against dimensionless speed of submersion. All measured volumes v were divided by a standard constant $v_0 = 67.2$ microliters. All submersion speeds were divided by the measured speed corresponding to the standard volume. For the plot below, $s_0 = 2.4$ mm/s.

Figure 25: Dimensionless bubble volume, v/v_0, plotted as a function of dimensionless submersion speed, s/s_0, where $v_0 = 59$ microliters and $s_0 = 2.4$ mm/s are used as the standard points by which the rest of the data is non dimensionalized. Fluid is tap water, with approximate surface tension of 72.4 mN/m, measurements taken in fluid of temperature between 20 and 24 degrees Celsius.

Uncertainty in volume measurement was calculated for a set of measurements taken at this speed. Average bubble volume at the 2.4 mm/s was 59 microliters with 4.9 microliters uncertainty. Uncertainty in terms of v/v_0 is 0.08.

The critical velocity is 2.4 mm/s. At speeds below 2.4 mm/s, corresponding to $s/s_0 = 1$ in the figure, bubble volume is within the range of uncertainty of the maximum. Between 2.4 and 6.3 mm/s, bubble volume decreases sharply. At submersion speeds above 6.3 mm/s of $s/s_0 = 2.6$, bubbles did not form in the device.

Many measurements were taken at low speeds. As the plot declines sharply quickly, the data was plotted with dimensionless volume versus the logarithm of the dimensionless speed. Figure 26 shows more detail in the first region of the plot, where submersion speed is below 4 mm/s and bubble volume is relatively constant at the maximum value.

Figure 26: Dimensionless bubble volume, v/v_0, plotted as a function of the logarithm dimensionless submersion speed, s/s_0, where $v_0 = 59$ microliters and $s_0 = 2.4$ mm/s are used as the standard points by which the rest of the data is non dimensionalized. Fluid is tap water, with approximate surface tension of 72.4 mN/m, measurements taken in fluid of temperature between 20 and 24 degrees Celsius.

The experiment was repeated in a fluid with 2.5% ethyl alcohol concentration, corresponding to a surface tension of 67.9 mN/m. In Figure 27, dimensionless bubble volume is plotted against dimensionless submersion speed for the 2.5% ethyl alcohol solution. For this set of data the standard volume was 43 microliters, while the standard speed was 1.7 mm/s. The standard volume was chosen because it was the maximum. The standard speed was the speed at which this volume was measured. Above $s/s_0 = 2$, decreasing v/v_0 is outside the range of error from testing.
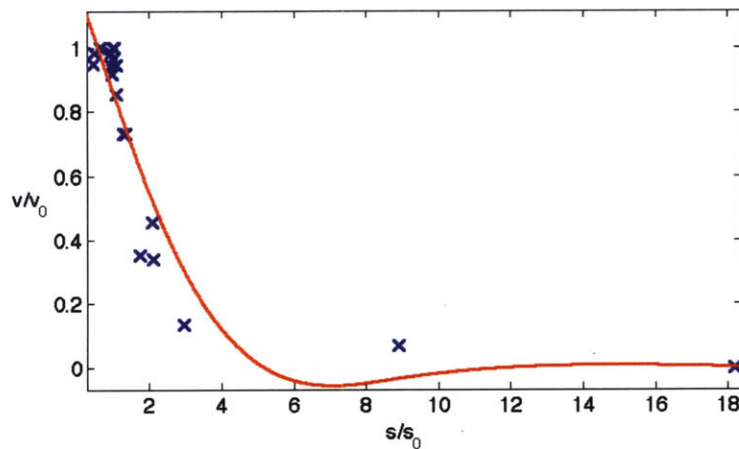
Figure 27: Dimensionless bubble volume, v/v_0, plotted as a function of dimensionless submersion speed, s/s_0, where $v_0 = 43$ microliters and $s_0 = 1.7$ mm/s are used as the standard points by which the rest of the data is non dimensionalized. Fluid is 2.5% ethyl alcohol in water, with approximate surface tension of 67.9 mN/m, measurements taken in fluid of temperature between 20 and 24 degrees Celsius.

The next plot, in Figure 28, is a plot of the same data, this time with dimensionless volume plotted against the logarithm of dimensionless speed for further illumination of trends in data.
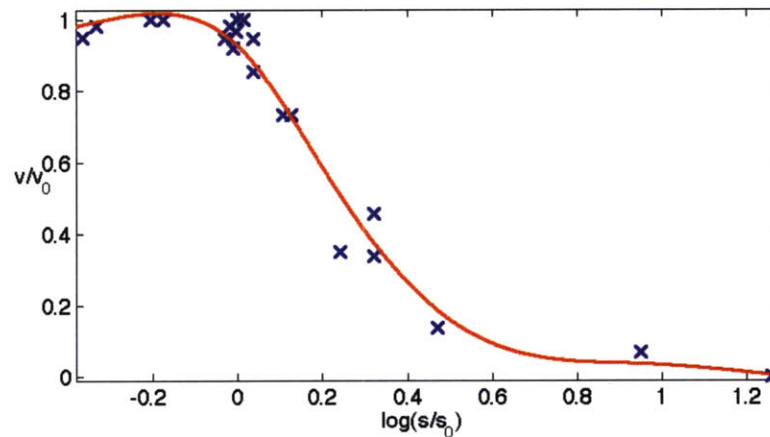

Figure 28: Dimensionless bubble volume, v/v_0, plotted as a function of the logarithm of dimensionless submersion speed, s/s_0, where $v_0 = 43$ microliters and $s_0 = 1.7$ mm/s are used as the standard points by which the rest of the data is non dimensionalized. Fluid is 2.5% ethyl alcohol in water, with approximate surface tension of 67.9, measurements taken in fluid of temperature between 20 and 24 degrees Celsius.

The experiment was repeated again, this time in a fluid with 5% ethyl alcohol concentration. Using the published surface tension data, this corresponds to a surface tension of 63.3 mN/m. In Figure 29, dimensionless bubble volume is plotted against dimensionless submersion speed for the 5% ethyl alcohol solution. For this set of data the standard volume was 36.5 microliters, while the standard speed was 1.6 mm/s. The standard speed was the speed at which this volume was measured. Again, above $s/s_0 = 2$, decreasing v/v_0 is outside the range of error from testing.
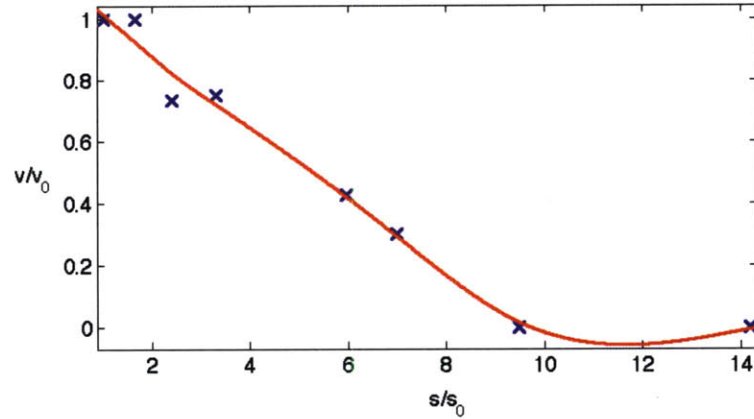
Figure 29: Dimensionless bubble volume, v/v_0, plotted as a function of dimensionless submersion speed, s/s_0, where $v_0 = 36.5$ microliters and $s_0 = 1.6$ mm/s are used as the standard points by which the rest of the data is non dimensionalized. Fluid is 5% ethyl alcohol in water, with approximate surface tension of 63.3 mN/m, measurements taken in fluid of temperature between 20 and 24 degrees Celsius.

The next plot, in Figure 30, is a plot of the same data, this time with dimensionless volume plotted against the logarithm of dimensionless speed for further illumination of trends in data.
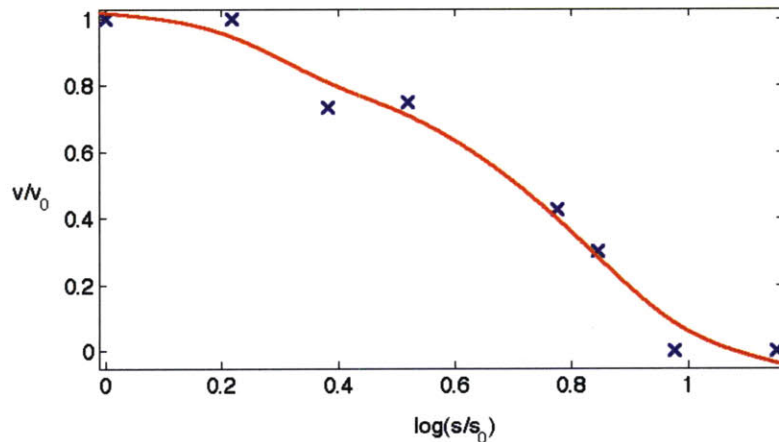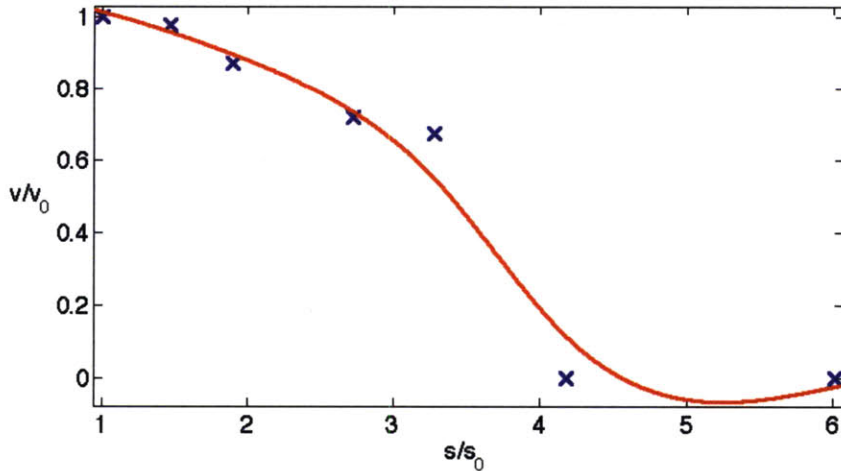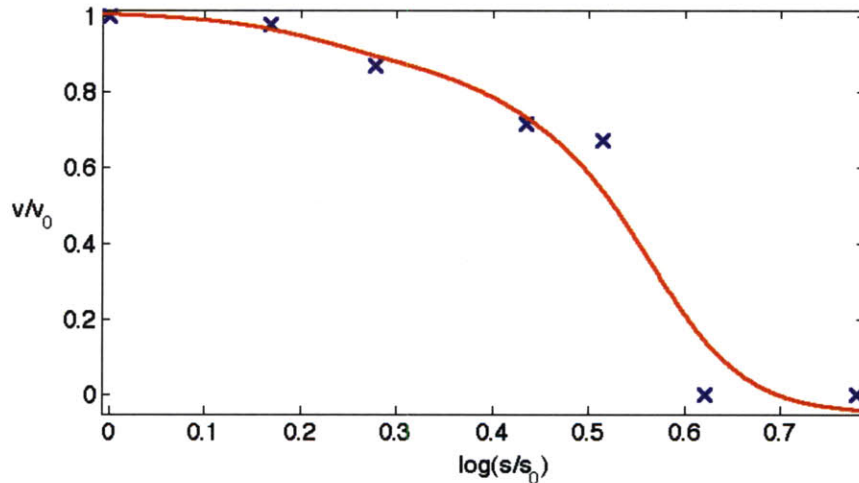

Figure 30: Dimensionless bubble volume, v/v_0, plotted as a function of the logarithm of dimensionless submersion speed, s/s_0, where $v_0 = 36.5$ microliters and $s_0 = 1.6$ mm/s are used as the standard points by which the rest of the data is non dimensionalized. Fluid is 2.5% ethyl alcohol in water, with approximate surface tension of 63.3, measurements taken in fluid of temperature between 20 and 24 degrees Celsius.

Unlike the two previous sets of data collected for 0% and 2.5% ethyl alcohol, bubble volume decreases very gradually. The table below summarizes the critical points and intervals in submersion speed plots.

Table 2: Comparative values of dimensionless submersion speed s/s_0 for the three regimes of bubble capture in fluids of varying ethyl alcohol concentration (0%, 2.5%, and 5%)

% Ethyl alcohol	s/s_0 for maximum bubble volume	s/s_0 for intermediate range – bubble volume rapidly decreasing	s/s_0 above which no bubbles form
0	0-1.5	1.5-9	9
2.5	0-2	2-10	10
5	0-1.5	1.5-4	4

Varying the submersion speed across fluids with three different surface tensions showed that there is a definite relationship between submersion speed and bubble volume. At speeds below approximately 2.4 mm/s bubble formation was at a maximum in all of the devices. Depending on the surface tension, this maximum was different, but maximum was achieved in the same speed range.

The submersion experiments also demonstrated that bubble volume has a varying relation with the submersion speed, depending on the speed regime. In the first regime, between zero and the first critical velocity, bubble volume is at a maximum. In this range, differences in speed contribute to negligible differences in volume. In the second regime, between the first critical velocity and a second critical velocity, bubble volumes drop quickly with increasing submersion velocity. Above the second critical velocity, there is no bubble capture. The results of this experiment show that submerging the device too quickly will result in no bubble being captured. Submerging slowly and steadily results in maximum bubble size.

The two lower concentrations, 0% and 2.5% were most similar in terms of speed intervals. Maximum bubble volume was obtained in approximately the same range of s/s_0 and the intermediate range was also approximately the same. When the fluid was 5% alcohol, behavior was slightly different. The range of s/s_0 for maximum bubble volume was essentially the same, but the intermediate range was much smaller. Bubbles stopped forming at a smaller s/s_0 than for the other two experiments. This may be because the interval between 2.5% and 5% alcohol concentration represents a decrease in surface tension that may be indicative of changed bubble behavior.

It is apparent from the v/v_0 vs $\log(s/s_0)$ plots that all data sets followed the same trend. At low speeds, bubble volume was relatively constant, followed be a sharp decline. This shows that the experimental methods were repeatable, and that altering surface tension did not completely change the behavior of the fluid with respect to the device. This last point is important when scaling the device for larger applications. Even though captured bubble volume was lower at lower surface tensions, behavior was still similar.

More data could be added to the submersion tests, could be expanded beyond the three ethyl alcohol concentrations, within the limit of 10% ethyl alcohol. It is likely not feasible to test smaller intervals between surface tension concentrations because error in testing would likely make results inconclusive.
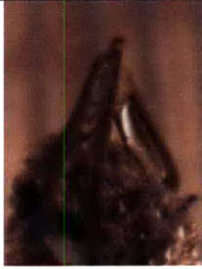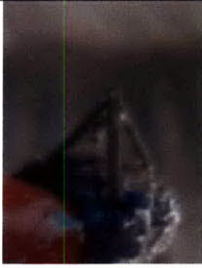
4.2.3 Qualitative Observations

The following table summarizes the results of the qualitative comparisons.

Table 3: Qualitative comparisons of device parameters (a) Hydrophobic coating on rods, (b) hydrophobic sponge, (c) number of rods, (d)

Condition		
a		
Coating on rods	Coated	Not coated
	Bubble forms, filling the frame of the device.	Bubbles form on the surface of the sponge, but no air is retained between the rods of the device.
b		
Hydrophobic sponge	Yes	No
	The bubble fills the frame of the device.	No retained bubble. Bubble collapses after bottom half of the device is submerged.
	Large	Small

	Bubble occupies only half the device, as the other half of the device is occupied by the sponge.	The bubble fills the frame of the device.
c		
Number of rods	2	3
	Meant to mimic the legs of the spider, no bubble formation.	
	4	5
		Bubble stays attached to longest, detaches right after device is submerged.
	6	

		The bubble fills the frame of the device.
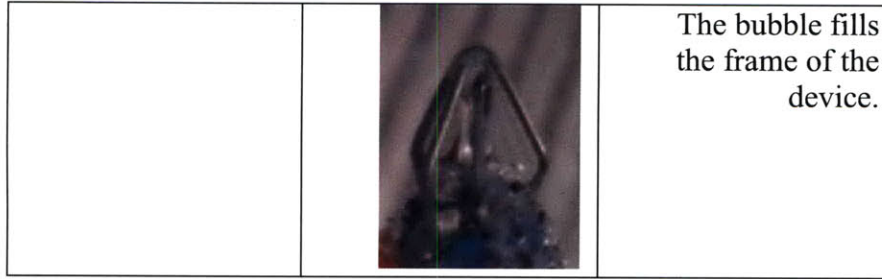
Hydrophobic coating on the rods was necessary for bubble capture. For future work, there are other ways to approach this problem. If surface roughness were applied to the rods on, potentially the rods could achieve the same level of hydrophobicity without adding in another layer. It would be desirable to eliminate the coating in favor of a surface features because this would eliminate any variability caused by the coating process. Surface roughening would increase the surface area of the rods. Objects with higher surface tension are more costly energetically to wet completely. Micron scale surface roughness could potentially prevent wetting.

The hydrophobic coating was applied to the rods to mimic the hydrophobic legs of the spider. The spider's legs are hairy, with hydrophobic oils. These characteristics are necessary for the water spider to use its legs as a frame for bubble capture and transport. If an application were to be developed, it might be preferred to eliminate the hydrophobic coating. The coating may wear off over time, decreasing the hydrophobicity of the surface. Hydrophobicity could be created through surface features.

The hydrophobic sponge is necessary for bubble formation, given the geometry of the device. The hydrophobic sponge was used to mimic the hairy hydrophobic abdomen of the spider. When the sponge takes up additional volume in the device, the bubble volume decreases correspondingly. A larger hydrophobic sponge could potentially be of use in a larger device. Finding the optimal scale requires much theory and calculation.

Six rods are necessary for bubble capture. When the device with five rods was submerged, the bubble stayed attached to all the rods up until the point at which the device became fully submerged in the water. In the other devices, the air did not fill the space between the rods completely. In these cases, the rods punctured the surface of the water much faster, becoming fully wetted. The water spider uses an active mechanism to separate the bubble from the surface, and only needs two legs to hold the bubble in place. The fact that the current mechanism is passive explains the discrepancy between number of rods and legs.

The selected parameters optimize the bubble volume for the given device. Under optimal conditions (six rods, hydrophobically coated rods, small hydrophobic sponge), the bubble fills the device, with curve interfaces projecting out from the device. The device can be modified to increase bubble volume further through a variety of steps.

5 Conclusion

The current study was inspired by the bubble capture techniques employed by the water spider. While observing videos of the water spider in its natural environment, the passive plastron that forms around the abdomen of the spider and more importantly, its ability to catch a large bubble of air and maintain it while it dives underwater prompted investigation into the characteristics of the water spider. We set out to mimic the mechanisms of the water spider by understanding the unique characteristics and behaviors it has developed for survival in an aquatic environment. In doing so methods for creating and maintaining a passive air layer on larger scale applications were illuminated.

5.1 Methods and Findings

In addressing this challenge, first bubble behavior was studied. Next, the mechanisms the water spider employs for bubble capture were more carefully examined and mimicked with a device inspired by the water spider. Finally, in this section, conclusions are drawn about the physics of bubble capture by the water spider and recommendations are given for developing larger scale applications. Implications of findings to real applications are also discussed.

The purpose of the nozzle experiments was to observe the effects of changing parameters of the basic experiment. The goal of changing these parameters was to increase the volume of the bubble before it would pinch off the nozzle.

The first conclusion to be drawn from the nozzle experiments is that bubble volume can be increased with simple modifications to the space above the nozzle opening. Given the system size constraint of the nozzle diameter, bubble volume was increased 15% above the volume that was emitted from simple underwater nozzle. The critical enhancement, a set of parallel rods placed vertically above the nozzle, was inspired by the legs of the water spider. This set of experiments showed that bubble volume can be passively increased through the proximity of simple geometric structures.

The findings from the rod nozzle experiments were applied to the creation of the bubble capture device. The development of this device was uncertain at first, as an active mechanism included much variability. A passive device was built, showing that the outcomes of the water spider's actions can be mimicked using readily available materials. The device was approximately the same size as the space created between the legs and abdomen of the water spider, and the corresponding bubbles for both were similar.

The development of the device alone can inspire much more future study. The water spider has not been used as inspiration in many other biomimicry projects, however much research can go into expanding on what has been found in the current study. Varying certain environmental parameters first gives a better understanding the of the water spider's behavior, so that its limitations and adaptations can be understood, but more importantly illuminates the possibilities for real applications.

The experiments examining the surface tension of the fluid and speed of submersion of the device give make clear constraints on a larger device, but at the same time show that it is possible to both capture and maintain a passive bubble layer on a larger scale surface.

Surface tension tests demonstrated that although bubble volume decreases when the surface tension of water is decreased, passive bubbles still form. A 25% surface tension decrease corresponds to a 50% decrease in bubble volume. In a larger scale device, when the surface tension is effectively smaller relative to the geometry of the device, given optimal geometry within the device, passive bubble formation is possible.

Speed of submersion experiments found that above a critical submersion speed bubbles did not form in the device, it is clear that there is a time dependence for bubble formation at this scale. Further investigation into a bubble capture device will have to take into account the fluid conditions where the device will be used. Additional experimentation could focus on the rate of fluid flow past the bubble capture device. This would explain why the water spider chooses low flow areas to build its habitat. It is hypothesized that in addition to the web staying intact outside of high flow areas, bubble formation is better in areas of low flow. Experimental results proving this hypothesis would increase the validity of the submersion speed experiments. Rate of fluid flow has been shown to affect bubbles emitted from an underwater nozzle (Gordillo 2005).

5.2 Insights

From the careful experimental investigations, it is shown that the water spider has optimized the capture of air despite a number of limitations. When expanding the bubble capture device to future applications, the necessary limitations set on the water spider must be considered. The water spider displays a delicate balance between bubble volume and body size. It must capture a large bubble to minimize the number of trips it must take to fill up its habitat. In order to capture a larger bubble, size of the spider must be increased. At the same time, making the trips to the water surface to capture bubbles is an energetically costly pursuit. The larger the water spider is, the more energy it expends in making the trip. In addition, the buoyancy forces that come along with a large bubble force the water spider to expend even more energy. The struggle the water spider undergoes is apparent in video footage of it capturing an air bubble. Bubble capture is fast, but the spider spends much more time just below the surface of the water, adjusting itself and aligning its legs to get as much energy as possible into swimming down into the water.

In creating an underwater application for the bubble capture mechanism, the additional energy due to buoyancy forces must be examined. It may be energetically too costly at a much larger scale to capture and maintain the required bubble size. The water spider may be close to the ideal geometry for the system. Additional research can go into finding the optimal balance between scale and bubble volume.

5.3 Future work

The most valuable thing learned from the water spider is about its limitations. Pinpointing the causes of all of these limitations and putting further study into working around them can lead to important innovations in artificial plastron creation.

In summary, further experimentation and theoretical work should go into the following areas to validate and expand upon the current conclusions:

1. Effect of fluid flow rate past the bubble capture device on the volume of the captured bubble

2. Study of geometry and optimal dimensions at the current scale

3. Theoretical scaling analysis based on geometry of the device and results of surface tension tests

4. Time dependence in bubble formation, both from an underwater nozzle and in bubble capture. More controlled experiments with submersion speed could examine the range that was outside the precision of the current study. This range was near zero speed.

5. Active mechanism that can be used to cut bubbles from the surface, in a more closely mimicked mechanism. This could potentially increase the volume of air that can be captured.

From there, the work can be expanded. A larger scale device that passively creates and maintains an air layer could be developed. This would be useful for underwater devices that require less drag, need to avoid corrosion, or require insulation. Using the water spider as inspiration and the conclusions drawn from the current study, real applications can be developed.

6 References

ARKive Images of Life on Earth. Water spider *(Argyroneta aquatica)*.
http://www.arkive.org/water-spider/argyroneta-aquatica/facts-and-status.html

Barthlott, W. and Neinhuis, C. 1997. Characterization and distribution of water repellent, self-cleaning plant surfaces. *Annals of Botany* 79: 667-677.

Burton, J. C., Waldrep, R. & Taborek, P. 2005. Scaling and instabilities in bubble pinch-off. *Phys. Rev. Lett.* 94, 184502.

Cassie, A. B. D. & Baxter, S. 1944. Wettability of porous surfaces. *Trans. Faraday Soc.* 40, 546–551.

Fontelos, M., Snoeijer, J., Eggers, J. 2009. The spatial structure of bubble pinch-off. *J. Fluid Mech.*

Flynn, R. and Bush, J. 2008. Underwater breathing: the mechanics of plastron respiration. *J. Fluid Mech.* 608, 275-296.

Gordillo, J. M., Sevilla, A., Rodriguez-Rodrigues, J. & Martinez-Bazan, C. 2005. Axisymmetric bubble pinch-off at high reynolds numbers. *Phys. Rev. Lett.* 95.

Herminghaus, S. 2000. Roughness-induced non-wetting. *Europhys. Lett.* 52, 165–170.

Kiriyanenko, A., Solov'ev, A. 1968. Measurement of the surface tension of alcohol-water solutions by the "two-jump" method. *Zhurnal Prikladnoi Mekhaniki i Tekhnicheskoi Fiziki.* 9, 145-148.

Keim, N. C., Møller, P., Zhang, W. W. & Nagel, S. R. 2006. Breakup of air bubbles in water: Memory and breakdown of cylindrical symmetry. *Phys. Rev. Lett.* 97, 144503.

Longuet, M., Kerman, B. and Lunde, K. 1991. The release of air bubbles from an underwater nozzle. *J. Fluid Mech.* 230: 365-390.

Oguz, H. N. & Prosperetti, A. 1993. Dynamics of bubble growth and detachment from a needle. *J. Fluid Mech.* 257, 111.

Ramé-Hart World Leader in Surface Science Instruments.
http://www.ramehart.com/goniometers/contactangle.htm.

Shirtcliffe, N. J., McHale, G., Newton, M. I., Perry, C. C. & Pyatt, F. Brian 2006. Plastron properties of a superhydrophobic surface. *Appl. Phys. Lett.* 89, 104106.

Schutz, D. and Taborsky, M. 2003. Adaptations to an aquatic life may be responsible for the reversed sexual size dimorphism in the water spider, *Argyroneta aquatica. Evolutionary Ecology Research* 5: 105-117.

Stephenson, R. 1997. Effects of oil and other surface-active organic pollutants on aquatic birds. *Environmental Conservation* 24, 121-129.

Thoroddsen, S. T., Etoh, E. G. & Takeara, K. 2007. Experiments on bubble pinch-off. *Phys. Fluids* 19, 042101.

Thorpe, W. H. 1950 Plastron respiration in aquatic insects. Biol. Rev. 25, 344–390.

WWLPT Biology Institute. Walking On Water: Water Striders and Surface Tension.
http://www.woodrow.org/teachers/bi/1998/waterstrider/student_lab.html